Multi-omics Approaches To Decipher the Impact of Diet and Host Physiology on the Mammalian Gut Microbiome

Deciphering the impact of diet and host physiology on the mammalian gut microbiome by multi-omics approaches

Running title: the mammalian gut microbiota and diet

Key words: microbiota, metagenomics, mammals, metatranscriptomics, diet, physiology

Christian Milani[2,4*], Giulia Alessandri[1*], Leonardo Mancabelli[2], Marta Mangifesta[2], Gabriele Andrea Lugli[2], Alice Viappiani[3], Giulia Longhi[3], Rosaria Anzalone[3], Sabrina Duranti[2], Francesca Turroni[2,4], Maria Cristina Ossiprandi[1,4], Douwe van Sinderen[5] and Marco Ventura[2,4]

*These authors contributed equally. Author order was defined based on seniority.

[1]Department of Veterinary Medical Science, University of Parma, Parma, Italy;

[2]Laboratory of Probiogenomics, Department of Chemistry, Life Sciences, and Environmental Sustainability, University of Parma, Parma, Italy;

[3]GenProbio srl, Parma, Italy;

[4]Microbiome Research Hub, University of Parma, Parma, Italy;

[5]APC Microbiome Institute and School of Microbiology, Bioscience Institute, National University of Ireland, Cork, Ireland

Correspondence. Mailing address for Marco Ventura Laboratory of Probiogenomics, Department of Chemistry, Life Sciences, and Environmental Sustainability, University of Parma, Parco Area delle Scienze 11a, 43124 Parma, Italy. Phone: ++39-521-905666. Fax: ++39-521-905604. E-mail: marco.ventura@unipr.it

Abstract

In recent years various studies have demonstrated that the gut microbiota influences host metabolism. However, these studies were primarily focused on a single or a limited range of host species, thus preventing a full exploration of possible taxonomic and functional adaptations by gut microbiota members as a result of host-microbe co-evolution events. In the current study, the microbial taxonomic profiles of 250 fecal samples, corresponding to 77 host species that cover the mammalian branch of the tree of life, were reconstructed by 16S rRNA gene-based sequence analysis. Moreover, shotgun metagenomics was employed to investigate the metabolic potential of the fecal microbiomes of 24 mammals and subsequent statistical analyses were performed to assess the impact of host diet and corresponding physiology of the digestive system on gut microbiota composition and functionality. Functional data was confirmed and extended through metatranscriptome assessment of gut microbial populations of eight animals, thus providing insights into the transcriptional response of gut microbiota to specific dietary lifestyles. Therefore, the analyses performed in this study support the notion that the metabolic features of the mammalian gut microbiota have adopted to maximize energy extraction from the host's diet.

Importance

Diet and host physiology have been recognized as main factors affecting both taxonomic composition and functional features of the mammalian gut microbiota. However, very few studies have investigated the bacterial biodiversity of mammals involving large sample numbers that correspond to multiple mammalian species, thus resulting in an incomplete understanding of the functional aspects of their microbiome. Therefore, we investigated the bacterial taxonomic composition of 250 fecal samples belonging to 77 host species distributed along the tree of life in order to assess how diet and host physiology impacts on the intestinal microbial community by selecting specific microbial players. Conversely, the application of shotgun metagenomics and metatranscriptomics approaches to a group of selected fecal samples allowed us to shed light on

both metabolic features and transcriptional responses of the intestinal bacterial community based on different diets.

Introduction

The functional roles exerted by the mammalian gut microbiota have in recent years been scrutinized by a range of studies focusing on multiple aspects of host biology, including the immune, digestive and nervous systems (1-4). In this regard, gut microbiota composition has been shown to be influenced by host genetics (5-11) as well as environmental factors that are linked to host lifestyle and diet (7, 10, 12-14). Microbe-host interactions are the result of intricate adaptive occurrences, through a process known as host-microbe co-evolution, being responsible for the adaptation of mammals to new environmental niches and having contributed to their dispersal and current global distribution (5, 15). Among multiple factors, diet, host evolutionary history and host physiology are currently presumed to be the main drivers implicated in the modulation of the mammalian gut microbiota (5, 7, 12, 13, 16-18). In this context, several comparative analyses of mammalian gut microbial communities have revealed associations between the composition of the gut ecosystem and host diet, even among phylogenetically un-related hosts (5, 18), and supported the notion that diet contributes to the microbiome plasticity by selecting particular metabolic activities to allow degradation of specific components of the host diet (5, 18, 19). Specifically, while carnivorous communities were reported to be specialized in the degradation of proteins, herbivorous microbiomes harbour genes which encode enzymatic activities involved in the breakdown of complex plant-derived polysaccharides, and absent in the genetic repertoire of their host, and which synthesize amino acid building blocks to cope with protein deficiency typical of their diet (18, 20, 21). In concert with diet, host phylogeny and physiology have been proposed as other crucial factors affecting the mammalian gut microbial community (5, 10, 16, 17). In recent years, the term ‘phylosymbiosis’ has been proposed to define the eco-evolutionary pattern that associates host evolutionary changes with ecological modulations of their intestinal microbial community (22, 23). Indeed, despite the inter-individual fluctuations of gut microbiomes and the possible rapid changes in response to diet and environment, it has been demonstrated that the mammalian gut microbiota

composition diverges at a relatively constant rate across an evolutionary timescale (10, 24), suggesting that host traits that undergo changes across host phylogeny, including gut physiology, have an important role in shaping the intestinal microbial community across mammals (7). However, this conserved pattern of host-microbe phylosymbiosis seems to be restricted to mammals. Indeed, meta-analysis performed on fecal samples of various bird, fish, reptile or amphibian species failed to report the same strict correlation (7, 16). Altogether, these findings indicate that the gut microbiota plays a pivotal role in facilitating adaptation to dietary changes adopted by mammals as part of their evolution, revealing particular correlations between a given gut microbiota and their associated host diet and/or digestive system (5, 7, 9, 10). Nevertheless, despite many studies depicting the gut microbiota as a hidden organ that exerts key metabolic activities to support its host, the composition and especially the functional role of mammalian gut microbial populations has not been fully explored. Indeed, despite the extensive number of mammalian species involved, most of the available studies explored the mammalian gut microbiota composition exclusively through 16S rRNA microbial profiling, thus failing to provide a correlation between the composition of the mammalian gut microbiota and its (predicted) metabolic functions (5, 7, 10, 16, 25). Other studies, even though they were based on shotgun metagenomics, did not investigate transcriptional profiles of the collected samples. In this context, in order to expand our knowledge in this field, the specific taxonomic and functional traits associated with different diets and physiology of the host's digestive system across the mammalian branch of the tree of life were assessed by means of metagenomics (16S rRNA microbial profiling and shotgun metagenomics) and metatranscriptomics approaches. Specifically, we collected fecal samples from 250 mammals, covering 77 species and representing a broad range of mammalian biodiversity. These samples were subjected to 16S rRNA gene microbial profiling in order to obtain an overview of the taxonomic composition of the gut microbiota among their mammalian hosts. Moreover, 24 key samples were subjected to shotgun metagenomic sequencing and reconstruction of their microbial metabolic

potential in order to identify features that allow adaptation to specific diets linked with various evolved physiologies of the mammalian gastrointestinal tract. These functional data were confirmed and integrated by data obtained by metatranscriptome analysis of eight animals, thereby providing insights into the transcriptional response of gut microbiota populations to specific diets.

Results and discussion

The gut microbiota biodiversity across the mammalian branch of the tree of life. We performed 16S rRNA gene-based microbial profiling of 250 fecal samples corresponding to 77 mammalian species, together forming a broad coverage of the mammalian tree of life (Table S1) (Supplementary Excel File 1). Specifically, the enrolled mammalian species represent 66 omnivores, 63 carnivores, 115 herbivores (encompassing different sub-classes accordingly to the physiology of their digestive tract) and 6 piscivores (Table 1). In this context, because of the difficulties in collecting multiple fecal samples from non-domesticated mammals, some of the fecal samples were collected from wild animals (i.e. wolves or boars) while others were retrieved from animals raised in captivity. Furthermore, difficulties in collecting fecal samples from aquatic mammals significantly restricted the number of piscivore members, being limited to two species of dolphins (three fecal samples per dolphin species) (Table S1). Illumina sequencing produced a total of 15,307,128 reads, with an average of 61,229 reads per sample. Evaluation of the alpha-diversity, i.e. the biodiversity of the bacterial population harboured by each sample, was performed through rarefaction curves representing the number of observed OTUs generated with 100 % identity cut-off and obtained for 10 sub-samplings of the total read pool. Average curves obtained for the 28 mammalian taxonomic families included in this study revealed that some herbivorous mammalian species, i.e. *Equidae*, *Camelidae*, *Macropodidae*, *Bovidae*, *Elephantidae* and *Giraffidae* possess a higher gut bacterial biodiversity compared to that of other mammals, supported by Student's t-test *p*-value of <0.001 (Figure 1a). This observation is confirmed by average diet-based rarefaction curves revealing a significantly higher biodiversity (Student's t-test *p*-value of <0.001) of the gut microbiota of herbivores when compared to that of omnivores or carnivores (the latter including piscivores) (Figure S1a). These data indicate that the overall bacterial biodiversity harboured by the mammalian gut positively correlates with the abundance of plant-based foods in the diet (*p*-value < 0.001), suggestive of a major metabolic role played by bacteria in the gastrointestinal tract of

herbivores. In this context, we also performed a sub-classification of the enrolled herbivores based on the physiology of their digestive system (Table S1) (Figure S1b). The average rarefaction curves that we obtained revealed that polygastric herbivores, including ruminants and pseudo-ruminants (Tylopoda), possess a significantly higher gut microbiota biodiversity (Figure S1b), reflecting the key role of foregut bacterial fermentation in herbivores with a multi-chambered stomach (26). The only exception was represented by *hippopotamidae* that showed lower biodiversity. Notably, this apparent inconsistency may reflect the peculiar physiology of the three-chambered stomach of these non-ruminant herbivores (26). In contrast, herbivores with single-chambered stomach showed significant variation in the number of observed OTUs based on their size (Figure S1b). In detail, 'lighter' (<100 Kg of average body weight) monogastric herbivores (representing five mammalian species and an associated total of 18 fecal samples) were shown to exhibit lower biodiversity when compared to that of 'heavier' (>100 Kg of average body weight) monogastric herbivores (encompassing eight mammalian species and a total of 32 fecal samples). This finding may reflect the fact that small herbivores are cecum fermenters, while heavier herbivores are colon fermenters (26). For this purpose, cecum fermenters possess an enlarged cecum, which retains small food particles for fermentation while fibrous and less digestible particles pass rapidly through the large intestine. This peculiar physiology of the gastrointestinal tract supports a high-fiber diet without the encumbrance of a large hindgut, thus being advantageous for small animals with high ratio of food intake with respect to their size (26). In contrast, in colon fermenters the content of colon and cecum mix freely and act as a single fermentation site (26), possibly supporting the higher bacterial biodiversity observed in heavier monogastric herbivores (Figure S1b).

Gut microbiota composition across the mammalian branch of the tree of life. Microbial taxonomic profiles obtained at genus level were used to perform a beta-diversity analysis using the Bray-Curtis distance matrix, and then represented by means of a PCoA plot (Figure 1b) (Figure

157 S2a). This analysis revealed clustering of samples based on taxonomic family, as expected, with
158 overlap of families with a similar diet (Figure S2a). In fact, re-colouring of the samples based on
159 dietary habits revealed that herbivores, omnivores and carnivores (including piscivores) clustered
160 separately (Figure 1b), with herbivores forming sub-clusters, confirming previously published
161 observations (18). In order to detail differences between herbivores, a specific Bray-Curtis PCoA
162 was generated (Figure S2b). The latter revealed three major clusters constituted by i) polygastric
163 ruminants and pseudo-ruminants (Tylopoda), ii) heavier monogastric herbivores, and iii) lighter
164 monogastric herbivores and *hippopotamidae* (Figure S2b). These findings highlight that diet, as
165 well as the physiology and anatomy of the herbivorous digestive system, not only impact on the
166 overall bacterial biodiversity, i.e., number of different bacterial taxa, but also on the gastrointestinal
167 microbiota composition.
168 Furthermore, in depth analysis of the microbial taxonomic profiles reconstructed from 16S rRNA
169 gene-based microbial profiling data evidenced similarities between taxonomic families of mammals
170 with an analogous diet (Figure 2a). Details regarding key taxa correlated with specific diets or
171 gastrointestinal physiologies are extensively discussed in the supplementary text. Amongst the most
172 relevant findings, it is worth mentioning that carnivores and herbivores are characterized by a
173 peculiarly high average abundance of the genus *Fusobacterium* and members of the
174 *Ruminococcaceae* family, respectively (Figure 2b). In this context, it has previously been shown
175 that the *Fusobacterium* genus is generally associated with a protein-rich diet (27), while a high
176 abundance of members of the *Ruminococcaceae* family is related to a fibre-based diet, since the
177 latter are degraders of a wide range of carbohydrates (28). Nevertheless, though our findings
178 indicate that members of these two bacterial taxonomic groups play a defining metabolic role for
179 their host, their sub-genus phylogeny and genetic potential are still poorly characterized. They
180 therefore represent prime targets for further genomic and functional studies. In this regard, analysis
181 of the herbivorous gut microbiota revealed that the *in silico* predicted genera UCG-005 and UCG-

010 of family *Ruminococcaceae* together represent 18.49 % of the total gut microbial population of polygastric herbivores (Figure S3a-b). Moreover, the small monogastric class (<100 Kg-average body weight) is characterized by a higher number of class-specific taxa when compared to other herbivores (Figure S3b), suggesting that the peculiar gut microbiota composition of cecum fermenters may reflect their shorter transit time and specific energy extraction capabilities when compared to colon fermenters, i.e. heavier monogastric animals (>100 Kg-body average weight), and ruminants (26).

Co-variance of gut colonizers across the mammalian tree of life. The composition and dynamics of the intestinal microbial community rely on an intricate cross-species network of interactions (29). In this context, previous studies have revealed the existence of both co-operative and competitive behaviours between members of the mammalian gut microbiota (29-31). In order to investigate such interactions that occur in the gut microbiota across all mammals, we performed a Kendall's tau coefficient co-variance analysis using all taxonomic profiles obtained in this study. Data collected were used to construct a force-driven network where attractive and repulsive forces between nodes correspond to positive and negative co-variances with a *p*-value of <0.05 between taxa for which a relative abundance of >5 % was observed in at least one sample (Figure 3a). In this context, colouring of the nodes based on modularity class analysis (resolution of 0.6) revealed the presence of three major clusters organised by co-occurring genera, a smaller cluster encompassing just four taxa and a single microbial genus that does not cluster with any of the other bacterial taxa (Figure 3a). Moreover, node colouring corresponding to taxa found to be associated with specific diets (p-value <0.05) (Figure 2) (Figure 3b) revealed that genera more abundant in herbivores, carnivores and piscivores clustered together, thus suggesting the existence of putative co-operational behaviours between these taxa. In contrast, genera found to be more abundant in omnivores are located near clusters associated with herbivores or carnivores, reflecting the mixed diet followed by

omnivorous mammals. This finding may indicate that omnivores are not associated with specific bacterial genera (or *vice versa*), but, rather, possess a combination of bacterial taxa typical of herbivores and carnivores. This notion is in accordance with a previous observation that omnivores do not possess 'generalist' bacterial lineages able to digest both plant- and animal-derived compounds but rather a combination of herbivorous and carnivorous specialist bacterial groups (25). In this milieu, it seems that diet may play a major role in modulating the mammalian gut microbiota, resulting in efficient metabolism of dietary food components.

To better detail differences between herbivores and carnivores, the nodes were also coloured to report genera showing higher relative abundance (p-value <0.05) in either of these two dietary groups (Table S2) (Figure 3c). Since the distance between nodes is weighted on statistically significant co-occurrence and co-exclusion interactions, this network analysis revealed that genera found to be more abundant in herbivores form a tighter cluster when compared to carnivore-specific taxa that are spread across the remaining area of the network (Figure 3c). On the basis of this finding, we speculate that bacterial genera involved in the metabolism of plant-derived carbohydrates need a higher level of co-operation to perform complete degradation of such complex carbohydrates, being abundant in the herbivorous diet, into simple sugars. This hypothesis is further supported by the higher average number of co-variances observed, as represented by node size, between herbivore-associated genera as compared to those corresponding to carnivores (Figure 3c).

Functional characterization of the mammalian gut microbiota. The 16S rRNA gene-based microbial profiling analysis revealed substantial differences in the taxonomic composition of the 250 collected fecal samples based on diet and physiology of the digestive system. For this reason, in order to trace potential differences in the functional repertoire of mammalian gut microbial populations, a shotgun metagenomic approach was performed for 24 fecal samples. Specifically, to obtain a balanced analysis, fecal samples were chosen in order to be equally divided per diet

category, with exclusion of omnivores due to their extreme complex and variable diet (Table S3). Furthermore, animals included in the same group were chosen randomly to cover multiple sampling sites in order to limit geographical biases. Data retrieved from shotgun sequencing comprised a total of 221,797,722 reads that were subjected to quality-filtering and removal of host-related sequences based on publicly available genomes of the sampled animals, resulting in a total of 205,386,184 reads with an average of 8,557,758 reads per sample (Table S3). The obtained sequence datasets were then subjected to metabolic pathway prediction based on the MetaCyc database. Shotgun metagenomics data revealed that the gut microbiota of piscivores encode the highest number of pathways (constituting an average of >0.001 % reads of the datasets) and a higher number of pathways with lower abundance compared to both other diets (Figure 4), thus allowing to formulate the hypothesis that aquatic life and correlated diet induced extensive shift in the metabolic potential of the gut microbiota of these piscivores (further details related to data collected from piscivores (dolphins) and their relative functional assessment are reported in Supplementary Text). Furthermore, statistical analysis revealed that carnivores possess a lower number of pathways with differential (higher or lower) abundance when compared to other diets (Bonferroni post-hoc test p-value <0.05) (Figure 4). In depth evaluation of degradative pathways showing higher abundance for a specific diet (Bonferroni post-hoc test p-value <0.05) (Figure 4) (Table S5) revealed, as expected, that the herbivore gut microbiome is enriched in carbohydrate degradation pathways when compared to that of carnivores and piscivores (Table S4). Particularly, most of the predicted pathways were related to the breakdown of typical plant carbohydrates, i.e. xylose, arabinose, sucrose, starch and maltose (32-34) (Table S5), predicting that the gut microbiome has a greater capacity to recover energy from a plant/vegetable-based diet. In contrast, the carnivore gut microbiome is characterized by a higher number of pathways related to choline degradation coupled with the super-pathway of trimethylamine degradation (Table S5). Notably, choline, a quaternary amine principally found in meats, is known as precursor of trimethylamine (35, 36). In this context,

the microbial intestinal community associated with carnivores seems to have developed activities capable of degrading meat components and its derived by-products, thus strengthening previous observations which suggested that the carnivore microbiome is specialized to derive energy from protein degradation (18). Collectively these findings support the notion that diet plays a role in modulating the taxonomic composition of the intestinal microbial community, with a consequent impact of the metabolic pathways encoded by these mammalian intestinal microbial communities.

Differences between the gut glycobiome of carnivores and herbivores. Shotgun metagenomic data were also used to reconstruct the glycobiome, i.e. the genetic repertoire responsible for breakdown of complex carbohydrates. Details of the variations in the gut microbiota glycobiome based on diet (herbivore, carnivore and piscivore) are reported in the Supplementary Text. Focusing on the comparison between the glycobiome profiles of carnivores and herbivores, we performed a Student's t-test statistical analysis. Results revealed that a large number of GH families possess differential abundance between the representatives of the two considered diets (Table S6). In this context, a marked commitment of carnivores was noticed towards the degradation of animal-derived host glycans and their degradation products (GH20, GH33, GH92, GH101, GH123, GH125 and GH129) as well as α(1→4) linked glucose polysaccharides (GH15, GH63 and GH126) such as the animal storage carbohydrate glycogen (Table S6). Moreover, carnivores showed higher abundance of GH families involved in the degradation of chitin, chitosan and chitobiose (GH19, GH23, GH84, GH85), probably due to the ingestion of chitinous structures (Table S6). In contrast, herbivore data extended the above observed specialization of their microbiota toward the metabolism of plant-related polysaccharides such as cellulose, xylans and galactans (GH9, GH10, GH11, GH12, GH16, GH26, GH31, GH39, GH42, GH43, GH44, GH51, GH53, GH67, GH74 and GH120) and highlighted also commitment toward degradation of fungal polysaccharides such as mycodextran (GH87) (Table S6).

Dissection and statistical analysis of glycobiome data revealed that the gut microbiomes of carnivores, piscivores and herbivores encode a specific repertoire of enzymes to allow energy extraction from dietary carbohydrates, suggesting that the bacterial populations harbored by the mammalian gut exert specific metabolic roles that are associated with the particular diet of their host.

Metatranscriptomic analysis of Carnivores and Herbivores microbiomes. Metagenomics data provided interesting information regarding functional commitment of the gut microbiota of herbivores and carnivores towards metabolism of specific dietary components. In order to evaluate if transcriptional profiles of these microbiomes reflect such observations, we performed metatranscriptome analysis of fecal samples from four carnivores and four herbivores (Table S7), which were selected in order to represent various animal genera. Sequenced metatranscriptome datasets were processed for removal of host DNA through mapping against a custom database of host genomes resulting in a total of 38,921,420 reads with an average of 4,865,177 reads per sample and the latter were further subjected to prediction of the expressed glycobiome and repertoire of degradation pathways (Table S5, Table S6 and Figure 5).

Inspection of transcriptional data revealed that the range of pathways involved in the breakdown of typical plant carbohydrates, i.e. xylose, arabinose and starch, found to be more abundant in herbivores based on shotgun metagenomic data (Table S5), are also more expressed in animals following this diet (Table S5). Similarly, analysis of the expressed glycobiomes focusing on GH families showing differential abundance in metagenomic data, evidenced that genetic members of the GH9, GH26, GH39, GH43, GH51, GH67 and GH74 glycosyl hydrolase families, predicted to be involved in the breakdown of plant-related carbohydrates, are more expressed in herbivores. In contrast, genes encoding GH20, GH33 and GH129 family enzymes, which are predicted to be involved in degradation of host-derived glycans, showed higher transcription levels in carnivores

(Table S6). Notably, these data further strengthen the assumption of an extensive specialization of the gut microbiota of mammals in facilitating the metabolism of specific dietary compounds in terms of the encoded genetic repertoire and being corroborated by their transcription patterns.

To further explore possible differential expression of metabolic pathways and GHs showing comparable abundance in metagenomic data collected from herbivores and carnivores, statistical analyses were extended to include all profiled pathways and GHs (Figure 5a). These analyses of transcriptomics data revealed that, compared to carnivores, herbivores are characterized by increased transcription of genes encoding a range of GH families involved in plant glycan degradation (Figure 5a). Among the latter, members of GH5 encompass cellulases, of GH97 include α-glucosidases and α-galactosidases, and enzymes belonging to GH130 are known to be involved in the breakdown of β-mannosides such as β-1,4-mannobiose. Furthermore, a range of degradation pathways involved in the metabolism of pectin, including its metabolites 4-deoxy-L-threo-hex-4-enopyranuronate, D-galacturonate and D-fructuronate, as well as the cell wall component L-rhamnose showed higher expression in herbivores (Figure 5a), despite comparable abundance of their corresponding genes in metagenomic datasets of carnivores. In addition, the super-pathway of methanogenesis showed higher expression in herbivores (Figure 5b), possibly reflecting the major metabolic role exerted by methanogens in this class of mammals (37).

Notably, metatranscriptome data allowed us to confirm functional data obtained from metagenomics approaches and provide insights into the transcriptional profiles of the gut microbial community of herbivores and carnivores in response to availability of specific dietary components. These findings may support the notion that intestinal microbial populations are able to differentially express genes in order to maximize food energy/nutrient extraction.

Exploration of functional specialization of the gut microbiome in classes of herbivores. Mammalian fecal samples that had been assessed by shotgun metagenome sequencing were selected

to cover the four main classes of herbivores depicted by analysis of 16S rRNA gene microbial profiling data, i.e. polygastric ruminants, polygastric pseudo-ruminants (Tylopoda), heavier monogastric herbivores (>100 Kg of average body weight) and lighter monogastric herbivores (<100 Kg of average body weight). Notably, comparison of the gut microbiome of polygastric ruminants and pseudo-ruminants revealed very limited differences in terms of encoded pathways and predicted glycobiome (Table S8 and Table S9). In detail, only one metabolic pathway with relative abundance >0.001 % was found to show increased abundance in ruminants ±50 % when compared to pseudo-ruminants (Student's t-test p-value <0.05), i.e. L-glutamate degradation IX (+72.89 %) (Table S8). Moreover, no degradation pathway classes showed statistically significant differential abundance. Notably, these data are consistent with the previously proposed notion that the gut microbiota of these two families of herbivores with a similar multi-chambered digestive system may exert comparable metabolic functions (26, 38). Indeed, comparison of the number of pathways with a statistically significant different abundance between the two groups of monogastric herbivores and ruminants or pseudo-ruminants revealed similar trends with the only exception of a slight decrease in the number of pathways with statistically significant higher abundance in the pseudo-ruminants when compared to monogastric herbivores (Table S10). For this reason, ruminants and pseudo-ruminants were considered as a single group for further comparison with heavier monogastric and lighter monogastric herbivores. Metabolic pathway prediction revealed that the total number of pathways with an abundance of >0.001 % and the number of degradative pathways with an abundance of >0.001 % is lower in polygastric animals when compared to monogastric herbivores.

Furthermore, our collected data revealed that the gut microbiota of ruminants and pseudo-ruminants encode the highest number of pathways with significant lower abundance when compared to monogastric herbivores (Figure 6), with a similar trend observed for degradative pathways (Figure 6). A possible explanation for these results is that the higher complexity of the digestive system of

polygastric herbivores requires less participation of gut microbiota in the associated catabolic processes when compared to the situation in monogastric mammals.

In contrast, the analysis of shotgun metagenomics data showed that the gut microbiota of lighter monogastric mammals encoded a more extensive repertoire of metabolic pathways (Figure 6). At the same time, as indicated above, 16S rRNA gene-based microbial profiling data revealed that lighter monogastric herbivores possess the lowest gut biodiversity among herbivores (p-value < 0.01)(Figure S1b), probably reflecting the limited colon size responsible for their specialization as cecum fermenters (26). On the basis of these two observations, it can be assumed that the intestinal bacterial community of lighter monogastric mammals compensates its reduced biodiversity by maximizing its metabolic potential when compared to heavy herbivores with a more complex digestive system.

In order to further explore peculiar catabolic capabilities of the enrolled classes of herbivores, a detailed evaluation of degradative metabolic pathways enriched in a specific class (ANOVA post-hoc Bonferroni p-value <0.05 when compared to either of the other groups) was performed (Table S10). Notably, the gut microbiota of the heavier monogastric herbivores revealed a specific commitment towards degradation of glycerol and a range of aromatic compounds including plant metabolites, such as 2, 3-dihydroxybenzoate, or environmental pollutants such as catechol, phenol and toluene (39-41) (Table S10). In contrast, the gut microbial population of lighter monogastric herbivores showed a specific abundance of pathways involved in the degradation of plant cell walls including hemicelluloses and their components, such as glucuronoarabinoxylan and galactans, pectin and rhamnogalacturonan along with reduction of the inorganic compound sulphate into hydrogen sulphide (Table S10). This observation may suggest that the higher biodiversity of heavier monogastric herbivores (Figure S1) supports specialization of gut commensals toward catabolism of a wider range of secondary plant-related compounds, while the less diverse gut microbial populations of lighter monogastric herbivores (Figure S1) appear more specialized to promote

efficient utilization of core plant saccharides. Furthermore, when considering polygastric herbivores, in addition to a higher abundance of pathways for degradation of simple sugars (mono- or di-saccharides) such as D- and L-arabinose, fucose, maltose, melibiose, trehalose and xylose, this herbivore class showed a higher abundance of a wide range of amino acid degradation pathways (Table S10). Notably, these results suggest that the mammalian gut microbiota plays a significant role in performing specific metabolic tasks not only dependent on host diet but also on the physiology of the corresponding digestive system.

Further exploration of the metabolic potential of herbivores through analysis of their glycobiome revealed that the microbiome of lighter monogastric herbivores encode the highest number of GH families at a significantly higher abundance (Table 3). Furthermore, five of the six GH families enriched in fecal material of lighter monogastric herbivores are either predicted to represent chitinase activity (associated with GH19), which participate in the hydrolysis of (1→4)-β-linkages between N-acetyl-D-glucosamine residues in the chitin-derived chitodextrins (GH25 and GH73), induce breakdown of 1,3-β-glucans (GH81) or encode broad spectrum β-glucosidases and β-mannosidases (GH1). In this context, all these predicted enzymatic activities may suggest a genetic specialization toward degradation of the main fungal cell wall components (42) (Table 3). Moreover, three of the four GH families enriched in heavier monogastric herbivores are involved in xylan degradation (GH54, GH116 and GH120) (Table 3).Therefore, these data may indicate that the gut microbiota of heavier monogastric herbivores has adapted to compensate for the reduced capability of these animals to metabolize complex plant saccharides when compared to polygastric ruminants. Furthermore, the abundance of GH family 79, which is enriched in polygastric herbivores (by 803 % and 3981 %) when compared to lighter and heavier monogastric herbivores, respectively (Table 3), is linked to the degradation of proteoglycans (such as arabinogalactan-linked proteins) (43, 44). Therefore, it seems that the gut microbiota of (pseudo)ruminants is involved in

maximizing energy extraction from food through improved breakdown of the extracellular matrix of plants.

Altogether these data reveal the relevant role of physiology and anatomy of the mammalian digestive system in order to co-operatively achieve optimal energy extraction from their particular diet.

Conclusions

A wide range of studies has suggested that diet and host physiology exert a crucial role in the modulation of both the taxonomical composition and metabolic repertoire of the mammalian gut microbiota. However, these studies did focus on specific diets and included a limited number of host species. For this reason, a precise dissection of the peculiar features that characterize the gut microbiota functionality in animals with specific dietary habits and an associated digestive system has so far not been performed. In the current study, the gut microbiota composition of 250 fecal samples, corresponding to 77 mammalian species, which broadly cover the mammalian branch of the tree of life, were explored through metagenomic approaches, encompassing 16S rRNA gene microbial profiling and shotgun metagenomics. Our results demonstrate that diet not only affects the intestinal microbial biodiversity but also the gut microbiota composition. In detail, 16S rRNA gene microbial profiling underlined existence of diet-associated genera, suggesting extensive co-evolution of gut bacteria with their hosts in order to promote selection of specific taxa. The finding that bacterial taxa typical of mammals following a specific diet co-occur in the gut environment supports this notion. Moreover, prediction of the metabolic potential of the gut microbial population of 24 mammals and metatranscriptome reconstruction of four carnivores and four herbivores revealed that the mammalian gut microbiome evolved to co-operate with its host digestive system from a functional point of view, strengthening the idea that the gut microbiota developed to optimize energy extraction from food. Indeed, among the herbivores, differences in the bacterial

biodiversity and taxonomical composition were observed when considering the physiology of their digestive system. These observations were further confirmed by comparison of the herbivore intestinal metabolic repertoire, showing that differences in the physiology of the digestive system correspond to diverse microbial metabolic capabilities. Altogether, these results suggest that mammalian gut microbiota has developed in order to achieve extensive metabolic interplay aimed at maximizing energy and nutrient extraction based on specific dietary habits. However, the difficulties in collecting a sufficient number of fecal samples to fully represent all the categories of diet and the anatomy of the digestive tract reported, affected the outcomes of the present study. In this context, the piscivore group is represented only by certain species of dolphins, thus limiting the acquired knowledge on the composition and metabolic repertoire of this group of animals. Furthermore, several samples were obtained from zoo animals whose microbial community may be affected by human influence and captivity. Therefore, further investigations aiming to retrieve fecal samples from a large cohort of piscivorous mammalian species as well as from mammals living in their natural environment are required to fully understand how the gut microbiota and its metabolic features co-evolved with the host. In addition, a follow-up study aimed at collecting fecal samples from different mammals at different time points may be useful to better assess whether the observed differences persist over time or if they are the results of transient shifts.

Materials and Methods

Ethics approval and consent to participate. All experimental procedures and protocols involving animals were approved by the Veterinarian Animal Care and Use Committee of Parma University, and conducted in accordance with the European Community Council Directives dated 22 September 2010 (2010/63/UE). Human participants gave their informed written consent before enrollment. All investigations were carried out following the principles of the Declaration of Helsinki.

Sample collection. A total of 250 stool samples were collected through a collaboration with several Italian zoological parks and farms. In case of aquatic mammals, sample collection was performed during a routine veterinary examination through rectal swabs to avoid contamination (Table S1). Conversely, for all other Terrestrial mammals, fecal samples were collected immediately after defecation. To be included in the study, animals had to be healthy, not having undergone treatment with any probiotics or drugs, such as antibiotics, during the six previous months (Table S1). In all cases, an aliquot of each fecal sample was transferred into a fecal container with RNAlater. All samples were kept on ice and shipped to laboratory under frozen conditions where they were preserved at -80 °C, until they were processed.

Bacterial DNA extraction, 16S rRNA gene PCR amplification and sequencing. Aliquots of fecal samples collected without RNAlater were subjected to bacterial DNA extraction using the QIAamp DNA Stool Mini Kit following the manufacturer's extraction (Qiagen). Partial 16S rRNA gene sequences were amplified from extracted DNA using primer pair Probio_Uni/Probio_Rev. targeting the V3 region of the 16S rRNA gene sequence (45). Illumina adapter overhang nucleotide sequences were added to the partial 16S rRNA gene-specific amplicons, which were further processed involving the 16S Metagenomic Sequencing Library Preparation Protocol (Part #15044223 Rev. B – Illumina). Amplifications were carried out using a Verity Thermocycler (Applied Biosystems). The integrity of the PCR amplicons was analyzed by electrophoresis on a 2200 TapeStation Instrument (Agilent Technologies, USA). DNA products obtained following PCR-mediated amplification of the 16S rRNA gene sequences were purified by a magnetic purification step employing the Agencourt AMPure XP DNA purification beads (Beckman Coulter Genomics GmbH, Bernried, Germany) in order to remove primer dimers. DNA concentration of the amplified sequence library was determined by a fluorometric Qubit quantification system (Life Technologies, USA). Amplicons were diluted to a concentration of 4 nM, and 5 µL quantities of

each diluted DNA amplicon sample were mixed to prepare the pooled final Library. Sequencing was performed using an Illumina MiSeq sequencer with MiSeq Reagent Kit v3 chemicals.

16S rRNA microbial profiling analysis. The .fastq files were processed using a custom script based on the QIIME software suite (46). Paired-end reads pairs were assembled to reconstruct the complete Probio_Uni / Probio_Rev amplicons. Quality control retained sequences with a length between 140 and 400 bp and mean sequence quality score >20 while sequences with homopolymers >7 bp and mismatched primers were omitted. In order to calculate downstream diversity measures (alpha and beta diversity indices, Unifrac analysis), 16S rRNA Operational Taxonomic Units (OTUs) were defined at 100 % sequence homology using DADA2 (47); OTUs not encompassing at least 2 sequences of the same sample were removed. Notably, this approach allows highly distinctive taxonomic classification at single nucleotide accuracy (46). All reads were classified to the lowest possible taxonomic rank using QIIME2 (46, 48) and a reference dataset from the SILVA database v.132 (49). Biodiversity within a given sample (alpha-diversity) was calculated considering the observed OTUs for 10 sub-samplings of the total read pool. Similarities between samples (beta-diversity) were calculated by unweighted/weighted uniFrac and Bray-Curtis (50). The range of similarities is calculated between values 0 and 1. PCoA representations of beta-diversity were performed using QIIME2 (46, 48).

Shotgun metagenomics. The extracted DNA was prepared following the Illumina Nextera XT DNA Library Preparation Kit. Briefly, the DNA samples were enzymatically fragmented, barcoded and purified involving magnetic beads. Then, samples were quantified using fluorometric Qubit quantification system (Life Technologies, USA), loaded on a 2200 Tape Station Instrument (Agilent Technologies, USA) and normalized to 4nM. Sequencing was performed using an Illumina NextSeq 500 sequencer with NextSeq High Output v2 Kit Chemicals 150 cycles.

Analysis of metagenomic datasets. The obtained fastq files were filtered for reads with a quality of < 25, for reads > 80 bp and for sequences of the mammalian host DNA. Moreover, bases were

removed from the end of the reads unless the average quality score was > 25, in a window of 5 bp. Only paired data were used to further analysis with METAnnotatorX using default settings (51). Investigation of Glycosyl Hydrolase (GH) profiles together with the reconstruction of bacterial metabolic pathways and evaluation of their abundance in the shotgun metagenomics datasets were assessed using custom scripts based on RapSearch2 software (52) and the CAZy database or the MetaCyc database (53), respectively.

RNA extraction. RNAlater-preserved stool samples were vortexed and homogenized after thawing for 10 min. Approximately 0.4 g of stool slurry was mixed with 1 mL of QIAzoL Lysis Reagent (Qiagen, UK) in a sterile tube containing glass beads (Merck, Germany). The cells were lysed alternating 2 minutes of stirring the mix on a Precellys 24 homogenizer (Bertin instruments, France) with 2 minutes of static cooling; this step was repeated three times. The lysed cells were centrifuged at 12,000 rpm for 15 min and the upper phase was recovered. The RNA samples were purified using the RNAesy Mini Kit (Qiagen, UK) following the manufacturer's protocol. RNA concentration and purity were evaluated by a Picodrop microliter spectrophotometer (Picodrop, UK).

RNAseq analysis performed by NextSeq Illumina. For RNA sequencing, 2.5 µg of total RNA was treated to remove ribosomal RNA by the Ribo-Zero Magnetic Kit (Illumina), followed by purification of the rRNA-depleted sample by ethanol precipitation. RNA was processed according to the manufacturer's protocol. The yield of rRNA depletion was checked by a Tape station 2200 (Agilent Technologies, USA). Then, a whole transcriptome library was constructed using the TruSeq Stranded RNA LT Kit (Illumina). Samples were loaded into a NextSeq High Output v2 Kit Chemicals 150 cycles (Illumina) as indicated by the technical support guide. The reads were depleted of adapters, quality filtered (with overall quality, quality window and length filters). Sequences corresponding to hosts' genomes where removed through mapping with bwa software (54) against a custom database of hosts' genomes. Retained reads were submitted to analysis with

METAnnotatorX tool (51). Investigation of Glycosyl Hydrolase (GH) profiles together with the reconstruction of bacterial metabolic pathways and evaluation of their abundance in the shotgun metagenomics datasets were assessed using custom scripts based on RapSearch2 software (Zhao et al 2012) and the CAZy database or the MetaCyc database (Caspi et al 2012), respectively.

Statistical analysis. All statistical analyses, i.e. ANOVA, PERMANOVA, Student's t-test as well as the Kendall tau rank co-variance analysis were performed with SPSS software v. 22 (IBM SPSS Statistics for Windows, Version 22.0. Armonk, NY: IBM Corp.). The force-driven network was created using Gephi (https://gephi.org/) and modularity was defined with resolution of 0.6.

Availability of data and materials. Raw sequences of 16S rRNA gene profiling data coupled with shotgun metagenomics and RNA sequencing data are accessible through SRA study accession number PRJNA545289 (https://www.ncbi.nlm.nih.gov/bioproject/545289) and PRJNA545214 (https://www.ncbi.nlm.nih.gov/bioproject/545214).

Funding

This work was primarily funded by the EU Joint Programming Initiative – A Healthy Diet for a Healthy Life (JPI HDHL, http://www.healthydietforhealthylife.eu/) to DvS (in conjunction with Science Foundation Ireland [SFI], Grant number 15/JP-HDHL/3280) and to MV (in conjunction with MIUR, Italy). The study is supported by Fondazione Cariparma, under TeachInParma Project (DV). GA is supported by Fondazione Cariparma, Parma, Italy. We furthermore thank GenProbio srl for financial support of the Laboratory of Probiogenomics.

Acknowledgements

This research benefited from the HPC (High Performance Computing) facility of the University of Parma, Italy. The authors declare that they have no competing interests. We thank 'Fondazione Bioparco di Roma' (Viale del Giardino Zoologico 20, 00197, Rome, Italy), 'Zoomarine' (Via dei

554 Romagnoli, 00040 Torvaianica, Pomezia, Rimini, Italy), 'Giardino Zoologico di Pistoia' (Via Pieve
555 a Celle, 160, 51100, Pistoia, Italy), 'Zoo Safari Ravenna' (Via dei Tre Lati 2x, 48125, Ravenna,
556 Località Mirabilandia-Savio di Ravenna, Italy), 'Centro Tutela e Ricerca Fauna Esotica e Selvatica
557 Monte Adone' (Via Brento, 9, 40037, Sasso Marconi, Bologna, Italy) and 'Parco Faunistico
558 Spormaggiore' (Via Nazionale, 38010 Spormaggiore, Trento, Italy) for their support in the
559 recruitment of the samples.

560 **Competing interests**

561 The authors declare that they have no competing interest.

References

1. McFall-Ngai M, Hadfield MG, Bosch TC, Carey HV, Domazet-Loso T, Douglas AE, Dubilier N, Eberl G, Fukami T, Gilbert SF, Hentschel U, King N, Kjelleberg S, Knoll AH, Kremer N, Mazmanian SK, Metcalf JL, Nealson K, Pierce NE, Rawls JF, Reid A, Ruby EG, Rumpho M, Sanders JG, Tautz D, Wernegreen JJ. 2013. Animals in a bacterial world, a new imperative for the life sciences. Proc Natl Acad Sci U S A 110:3229-36.
2. Tremaroli V, Backhed F. 2012. Functional interactions between the gut microbiota and host metabolism. Nature 489:242-9.
3. Round JL, Mazmanian SK. 2009. The gut microbiota shapes intestinal immune responses during health and disease. Nat Rev Immunol 9:313-23.
4. Diaz Heijtz R, Wang S, Anuar F, Qian Y, Bjorkholm B, Samuelsson A, Hibberd ML, Forssberg H, Pettersson S. 2011. Normal gut microbiota modulates brain development and behavior. Proc Natl Acad Sci U S A 108:3047-52.
5. Ley RE, Hamady M, Lozupone C, Turnbaugh PJ, Ramey RR, Bircher JS, Schlegel ML, Tucker TA, Schrenzel MD, Knight R, Gordon JI. 2008. Evolution of mammals and their gut microbes. Science 320:1647-51.
6. Goodrich JK, Waters JL, Poole AC, Sutter JL, Koren O, Blekhman R, Beaumont M, Van Treuren W, Knight R, Bell JT, Spector TD, Clark AG, Ley RE. 2014. Human genetics shape the gut microbiome. Cell 159:789-99.
7. Song SJ, Sanders JG, Delsuc F, Metcalf J, Amato K, Taylor MW, Mazel F, Lutz HL, Winker K, Graves GR, Humphrey G, Gilbert JA, Hackett SJ, White KP, Skeen HR, Kurtis SM, Withrow J, Braile T, Miller M, McCracken KG, Maley JM, Ezenwa VO, Williams A, Blanton JM, McKenzie VJ, Knight R. 2020. Comparative Analyses of Vertebrate Gut Microbiomes Reveal Convergence between Birds and Bats. mBio 11.
8. Goodrich JK, Davenport ER, Clark AG, Ley RE. 2017. The Relationship Between the Human Genome and Microbiome Comes into View. Annu Rev Genet 51:413-433.
9. Gaulke CA, Arnold HK, Humphreys IR, Kembel SW, O'Dwyer JP, Sharpton TJ. 2018. Ecophylogenetics Clarifies the Evolutionary Association between Mammals and Their Gut Microbiota. mBio 9.
10. Nishida AH, Ochman H. 2018. Rates of gut microbiome divergence in mammals. Mol Ecol 27:1884-1897.
11. Benson AK. 2015. Host genetic architecture and the landscape of microbiome composition: humans weigh in. Genome Biol 16:203.
12. Carmody RN, Gerber GK, Luevano JM, Jr., Gatti DM, Somes L, Svenson KL, Turnbaugh PJ. 2015. Diet dominates host genotype in shaping the murine gut microbiota. Cell Host Microbe 17:72-84.
13. David LA, Maurice CF, Carmody RN, Gootenberg DB, Button JE, Wolfe BE, Ling AV, Devlin AS, Varma Y, Fischbach MA, Biddinger SB, Dutton RJ, Turnbaugh PJ. 2014. Diet rapidly and reproducibly alters the human gut microbiome. Nature 505:559-63.
14. Alessandri G, Milani C, Mancabelli L, Mangifesta M, Lugli GA, Viappiani A, Duranti S, Turroni F, Ossiprandi MC, van Sinderen D, Ventura M. 2019. The impact of human-facilitated selection on the gut microbiota of domesticated mammals. FEMS Microbiol Ecol 95.
15. Moran NA. 2006. Symbiosis. Curr Biol 16:R866-71.
16. Youngblut ND, Reischer GH, Walters W, Schuster N, Walzer C, Stalder G, Ley RE, Farnleitner AH. 2019. Host diet and evolutionary history explain different aspects of gut microbiome diversity among vertebrate clades. Nat Commun 10:2200.
17. Amato KR, J GS, Song SJ, Nute M, Metcalf JL, Thompson LR, Morton JT, Amir A, V JM, Humphrey G, Gogul G, Gaffney J, A LB, G AOB, F PC, Di Fiore A, N JD, T LG, Gomez A, Kowalewski MM, R JL, Link A, M LS, Tecot S, B AW, K EN, R MS, Knight R, S RL. 2019. Evolutionary trends in host physiology outweigh dietary niche in structuring primate gut microbiomes. ISME J 13:576-587.

18. Muegge BD, Kuczynski J, Knights D, Clemente JC, Gonzalez A, Fontana L, Henrissat B, Knight R, Gordon JI. 2011. Diet drives convergence in gut microbiome functions across mammalian phylogeny and within humans. Science 332:970-4.
19. Kohl KD, Weiss RB, Cox J, Dale C, Dearing MD. 2014. Gut microbes of mammalian herbivores facilitate intake of plant toxins. Ecol Lett 17:1238-46.
20. Ley RE, Lozupone CA, Hamady M, Knight R, Gordon JI. 2008. Worlds within worlds: evolution of the vertebrate gut microbiota. Nat Rev Microbiol 6:776-88.
21. Russell JB, Rychlik JL. 2001. Factors that alter rumen microbial ecology. Science 292:1119-22.
22. Brooks AW, Kohl KD, Brucker RM, van Opstal EJ, Bordenstein SR. 2016. Phylosymbiosis: Relationships and Functional Effects of Microbial Communities across Host Evolutionary History. PLoS Biol 14:e2000225.
23. Sanders JG, Powell S, Kronauer DJ, Vasconcelos HL, Frederickson ME, Pierce NE. 2014. Stability and phylogenetic correlation in gut microbiota: lessons from ants and apes. Mol Ecol 23:1268-83.
24. Moeller AH, Li Y, Mpoudi Ngole E, Ahuka-Mundeke S, Lonsdorf EV, Pusey AE, Peeters M, Hahn BH, Ochman H. 2014. Rapid changes in the gut microbiome during human evolution. Proc Natl Acad Sci U S A 111:16431-5.
25. Groussin M, Mazel F, Sanders JG, Smillie CS, Lavergne S, Thuiller W, Alm EJ. 2017. Unraveling the processes shaping mammalian gut microbiomes over evolutionary time. Nat Commun 8:14319.
26. Dehority BA. 2002. Gastrointestinal tracts of herbivores, particularly the ruminant: Anatomy, physiology and microbial digestion of plants. Journal of Applied Animal Research 21:145-160.
27. Vital M, Gao J, Rizzo M, Harrison T, Tiedje JM. 2015. Diet is a major factor governing the fecal butyrate-producing community structure across Mammalia, Aves and Reptilia. ISME J 9:832-43.
28. La Reau AJ, Suen G. 2018. The Ruminococci: key symbionts of the gut ecosystem. J Microbiol 56:199-208.
29. Coyte KZ, Rakoff-Nahoum S. 2019. Understanding Competition and Cooperation within the Mammalian Gut Microbiome. Curr Biol 29:R538-R544.
30. Garcia-Bayona L, Comstock LE. 2018. Bacterial antagonism in host-associated microbial communities. Science 361.
31. Milani C, Mangifesta M, Mancabelli L, Lugli GA, James K, Duranti S, Turroni F, Ferrario C, Ossiprandi MC, van Sinderen D, Ventura M. 2017. Unveiling bifidobacterial biogeography across the mammalian branch of the tree of life. ISME J 11:2834-2847.
32. Kotake T, Yamanashi Y, Imaizumi C, Tsumuraya Y. 2016. Metabolism of L-arabinose in plants. J Plant Res 129:781-792.
33. Milani C, Lugli GA, Duranti S, Turroni F, Mancabelli L, Ferrario C, Mangifesta M, Hevia A, Viappiani A, Scholz M, Arioli S, Sanchez B, Lane J, Ward DV, Hickey R, Mora D, Segata N, Margolles A, van Sinderen D, Ventura M. 2015. Bifidobacteria exhibit social behavior through carbohydrate resource sharing in the gut. Sci Rep 5:15782.
34. Jones SA, Jorgensen M, Chowdhury FZ, Rodgers R, Hartline J, Leatham MP, Struve C, Krogfelt KA, Cohen PS, Conway T. 2008. Glycogen and maltose utilization by Escherichia coli O157:H7 in the mouse intestine. Infect Immun 76:2531-40.
35. Wang Z, Bergeron N, Levison BS, Li XS, Chiu S, Jia X, Koeth RA, Li L, Wu Y, Tang WHW, Krauss RM, Hazen SL. 2019. Impact of chronic dietary red meat, white meat, or non-meat protein on trimethylamine N-oxide metabolism and renal excretion in healthy men and women. Eur Heart J 40:583-594.
36. Rath S, Heidrich B, Pieper DH, Vital M. 2017. Uncovering the trimethylamine-producing bacteria of the human gut microbiota. Microbiome 5:54.
37. Enzmann F, Mayer F, Rother M, Holtmann D. 2018. Methanogens: biochemical background and biotechnological applications. AMB Express 8:1.
38. Al-Masaudi S, El Kaoutari A, Drula E, Redwan EM, Lombard V, Henrissat B. 2019. A metagenomics investigation of carbohydrate-active enzymes along the goat and camel intestinal tract. Int Microbiol 22:429-435.

39. Aghapour AA, Moussavi G, Yaghmaeian K. 2013. Biological degradation of catechol in wastewater using the sequencing continuous-inflow reactor (SCR). J Environ Health Sci Eng 11:3.
40. Kahru A, Maloverjan A, Sillak H, Pollumaa L. 2002. The toxicity and fate of phenolic pollutants in the contaminated soils associated with the oil-shale industry. Environ Sci Pollut Res Int Spec No 1:27-33.
41. Kim HJ, Choi SW, Inyang HI. 2008. Catalytic oxidation of toluene in contaminant emission control systems using Mn-Ce/gamma-Al2O3. Environ Technol 29:559-69.
42. Adams DJ. 2004. Fungal cell wall chitinases and glucanases. Microbiology 150:2029-35.
43. Nothnagel EA. 1997. Proteoglycans and related components in plant cells. Int Rev Cytol 174:195-291.
44. Du H, Clarke AE, Bacic A. 1996. Arabinogalactan-proteins: A class of extracellular matrix proteoglycans involved in plant growth and development. Trends in Cell Biology 6:411-414.
45. Milani C, Hevia A, Foroni E, Duranti S, Turroni F, Lugli GA, Sanchez B, Martin R, Gueimonde M, van Sinderen D, Margolles A, Ventura M. 2013. Assessing the fecal microbiota: an optimized ion torrent 16S rRNA gene-based analysis protocol. PLoS One 8:e68739.
46. Caporaso JG, Kuczynski J, Stombaugh J, Bittinger K, Bushman FD, Costello EK, Fierer N, Pena AG, Goodrich JK, Gordon JI, Huttley GA, Kelley ST, Knights D, Koenig JE, Ley RE, Lozupone CA, McDonald D, Muegge BD, Pirrung M, Reeder J, Sevinsky JR, Turnbaugh PJ, Walters WA, Widmann J, Yatsunenko T, Zaneveld J, Knight R. 2010. QIIME allows analysis of high-throughput community sequencing data. Nat Methods 7:335-6.
47. Callahan BJ, McMurdie PJ, Rosen MJ, Han AW, Johnson AJ, Holmes SP. 2016. DADA2: High-resolution sample inference from Illumina amplicon data. Nat Methods 13:581-3.
48. Bokulich NA, Kaehler BD, Rideout JR, Dillon M, Bolyen E, Knight R, Huttley GA, Gregory Caporaso J. 2018. Optimizing taxonomic classification of marker-gene amplicon sequences with QIIME 2's q2-feature-classifier plugin. Microbiome 6:90.
49. Quast C, Pruesse E, Yilmaz P, Gerken J, Schweer T, Yarza P, Peplies J, Glockner FO. 2013. The SILVA ribosomal RNA gene database project: improved data processing and web-based tools. Nucleic Acids Res 41:D590-6.
50. Lozupone C, Knight R. 2005. UniFrac: a new phylogenetic method for comparing microbial communities. Appl Environ Microbiol 71:8228-35.
51. Milani C, Casey E, Lugli GA, Moore R, Kaczorowska J, Feehily C, Mangifesta M, Mancabelli L, Duranti S, Turroni F, Bottacini F, Mahony J, Cotter PD, McAuliffe FM, van Sinderen D, Ventura M. 2018. Tracing mother-infant transmission of bacteriophages by means of a novel analytical tool for shotgun metagenomic datasets: METAnnotatorX. Microbiome 6:145.
52. Zhao Y, Tang H, Ye Y. 2012. RAPSearch2: a fast and memory-efficient protein similarity search tool for next-generation sequencing data. Bioinformatics 28:125-6.
53. Caspi R, Altman T, Dreher K, Fulcher CA, Subhraveti P, Keseler IM, Kothari A, Krummenacker M, Latendresse M, Mueller LA, Ong Q, Paley S, Pujar A, Shearer AG, Travers M, Weerasinghe D, Zhang P, Karp PD. 2012. The MetaCyc database of metabolic pathways and enzymes and the BioCyc collection of pathway/genome databases. Nucleic Acids Res 40:D742-53.
54. Li H, Durbin R. 2009. Fast and accurate short read alignment with Burrows-Wheeler transform. Bioinformatics 25:1754-60.

Tables

Table 1: list of mammals whose fecal samples were collected for this study, including the number of sampled individuals per mammalian species and their diets.

Common name	Species	Family	Number of sampled individuals	Diet group
African moufflon	*Ammotragus lervia*	Bovidae	2	Herbivore (Polygastric Ruminant)
European bison	*Bison bonasus*	Bovidae	2	
Banteng	*Bos javanicus*	Bovidae	1	
Auroch	*Bos primigenius*	Bovidae	1	
Cow	*Bos taurus*	Bovidae	16	
Goat	*Capra aegagrus hircus*	Bovidae	1	
Goat	*Capra hircus*	Bovidae	4	
Nile lechwe	*Kobus megaceros*	Bovidae	1	
Sheep	*Ovis aries*	Bovidae	4	
Mouflon	*Ovis musimon*	Bovidae	5	
Eland	*Taurotragus oryx*	Bovidae	1	
Deer	*Capreolus capreolus*	Cervidae	1	
Giraffe	*G. camelopardalis*	Giraffidae	2	
Camel	*Camelus bactrianus*	Camelidae	2	Herbivore (Polygastric Tylopoda)
Llama	*Lama glama*	Camelidae	1	
Guanaco	*Lama guanicoe*	Camelidae	3	
Alpaca	*Vicugna pacos*	Camelidae	7	
Vicuna	*Vicugna vicugna*	Camelidae	1	
Pygmy hippopotamus	*Hexaprotodon liberiensis*	Hippopotamidae	5	Herbivore (Polygastric Non-Ruminant 3 Stomach)
Hippopotamus	*Hippopotamus amphibius*	Hippopotamidae	3	
Grey kangaroo	*Macropus giganteus*	Macropodidae	1	
Hare	*Lepus europaeus*	Leporidae	9	Herbivore (Monogastric <100 kg)
European rabbit	*Oryctolagus cuniculus*	Leporidae	4	
European beaver	*Castor fiber*	Castoridae	2	
Patagonian mara	*Dolichotis patagonum*	Caviidae	1	
Capybara	*Hydrochoerus hydrochaeris*	Caviidae	2	
African wild donkey	*Equus africanus*	Equidae	4	Herbivore (Monogastric >100 kg)
Donkey	*Equus africanus asinus*	Equidae	5	
Wild horse	*Equus ferus*	Equidae	3	
Horse	*Equus ferus caballus*	Equidae	10	
Grevy zebra	*Equus grevyi*	Equidae	2	
Zebra	*Equus quagga*	Equidae	2	
Asiatic tapir	*Tapirus indicus*	Tapiridae	1	
Sudamerican tapir	*Tapirus terrestris*	Tapiridae	3	
Asiatic elephant	*Elephas maximus*	Elephantidae	2	
Wolf	*Canis lupus*	Canidae	10	Carnivore
Dog	*Canis lupus familiaris*	Canidae	25	
African wild dog	*Lycaon pictus*	Canidae	1	
Wil cat	*Felis silvestris*	Felidae	2	
Cat	*Felis silvestris catus*	Felidae	4	
European lynx	*Lynx lynx*	Felidae	1	
Lion	*Panthera leo*	Felidae	2	
Asiatic lion	*Panthera leo persica*	Felidae	1	
Jaguar	*Panthera onca*	Felidae	1	

Leopard	*Panthera pardus*	Felidae	1	
Tiger	*Panthera tigris*	Felidae	3	
Meerkat	*Suricata suricatta*	Herpestidae	1	
Fur seal	*Arctocephalus pussilus pussilus*	Otariidae	1	
Sudamerican sea lion	*Otaria flavescens*	Otariidae	1	
Grey seal	*Halichoerus grypus*	Phocidae	2	
Red coati	*Nasua nasua*	Procyonidae	1	
Brown bear	*Ursus arctos*	Ursidae	4	
Armadillo	*Chaetophractus villosus*	Dasypodidae	2	
Hedgehog	*Erinaceus europaeus*	Erinaceidae	1	
Wild boar	*Sus scrofa*	Suidae	8	Omnivore
Pig	*Sus scrofa domesticus*	Suidae	10	
Pygmy marmoset	*Callithrix pygmaea*	Cebidae	1	
Emperor tamarins	*Saguinus imperator*	Cebidae	1	
Cotton-top tamarin	*Saguinus oedipus*	Cebidae	1	
Saimiri	*Saimiri boliviensis peruviensis*	Cebidae	1	
Goeldi tamarin	*Callimico goeldii*	Cebidae	1	
Collared mangbey	*Cercocebus torquatus*	Cercopithecidae	1	
Green cercopithecus	*Chlorocebus pygerythrus*	Cercopithecidae	1	
Red-faced macaque	*Macaca fuscata*	Cercopithecidae	1	
Mandrill	*Mandrillue sphinx*	Cercopithecidae	1	
Human	*Homo Sapiens*	Hominidae	19	
Chimpanzee	*Pan troglodytes*	Hominidae	1	
Bornean orangutan	*Pongo pygmaeus*	Hominidae	1	
Macaque	*Eulemur macaco*	Lemuridae	1	
Lemur	*Lemur catta*	Lemuridae	2	
Red ruffed lemur	*Varecia rubra*	Lemuridae	1	
Black-and-white ruffed lemur	*Varecia variegata*	Lemuridae	1	
Wood mouse	*Apodemus sylvaticus*	Muridae	5	
Mouse	*Mus musculus*	Muridae	2	
Rat	*Rattus rattus*	Muridae	6	
Dolphin	*Delphinus delphis*	Delphinidae	3	Piscivore
Bottlenose dolphin	*Tursiops truncatus*	Delphinidae	3	

719 **Table 2:** List of GH families with statistically significant higher or lower abundance based on diet.

GH family	Carnivores	Piscivores	Herbivores
GH2	9.11%	**1.98%**	8.01%
GH3	4.65%	**1.35%**	5.47%
GH9	0.10%	0.25%	**0.68%**
GH10	0.18%	0.10%	**0.57%**
GH17	0.02%	**0.59%**	0.00%
GH19	0.04%	**0.30%**	0.01%
GH20	**2.54%**	1.04%	1.46%
GH23	1.95%	**13.36%**	1.04%
GH24	**0.23%**	0.05%	0.11%
GH26	0.16%	0.00%	**0.30%**
GH27	0.25%	0.05%	**0.57%**
GH29	1.52%	**0.57%**	1.43%
GH31	1.97%	**0.80%**	**2.57%**
GH33	0.79%	0.62%	**0.30%**
GH35	0.57%	**0.09%**	0.53%
GH39	0.01%	0.00%	**0.15%**
GH43	2.48%	0.48%	**4.14%**
GH51	0.60%	0.30%	**1.69%**
GH53	0.05%	0.08%	**0.31%**
GH67	0.09%	0.00%	**0.29%**
GH74	0.00%	0.00%	**0.08%**
GH100	**0.01%**	0.00%	0.00%
GH102	0.05%	**0.29%**	0.03%
GH103	0.05%	**0.42%**	0.03%
GH110	0.16%	**5.66%**	0.10%
GH129	**0.05%**	0.00%	0.01%
GH130	0.54%	**0.00%**	0.55%

720 *percentages in bold indicate Bonferroni post-hoc test p-value <0.05 when compared to other
721 groups.

722 **Table 3:** List of GH families with statistically significant higher or lower abundance based on
723 digestive system's physiology.

GH family	Heavier Monogastric	Lighter Monogastric	Polygastric
GH1	0.0066%	**0.0150%**	0.0075%
GH4	0.0056%	0.0038%	**0.0146%**
GH19	0.0001%	**0.0005%**	0.0001%
GH25	0.0041%	**0.0082%**	0.0048%
GH32	0.0048%	**0.0106%**	0.0051%
GH38	0.0051%	0.0039%	**0.0103%**
GH50	**0.0010%**	0.0004%	0.0004%
GH54	**0.0010%**	0.0000%	0.0001%
GH73	0.0067%	**0.0157%**	0.0061%
GH79	0.0001%	0.0003%	**0.0026%**
GH81	0.0000%	**0.0002%**	0.0001%
GH116	**0.0032%**	0.0007%	0.0008%
GH120	**0.0066%**	**0.0012%**	0.0030%

724 *percentages in bold indicate Bonferroni post-hoc test p-value <0.05 when compared to other
725 groups.

726 **Figure legends**

727

728 **Figure 1.** Alpha and Beta diversity of mammals included in this study. Panel a shows the average
729 rarefaction curves obtained for each mammalian taxonomic family through evaluation of the
730 number of observed OTUs up to 30,000 reads. Panel b reports the PCoA representation obtained
731 using the Bray-Curtis index and the genus-level profiles. Samples were colored based on diet, i.e.
732 carnivores, herbivores, piscivores and omnivores.

733

734 **Figure 2.** Impact of diet on mammalian gut microbiota genus-level taxonomic composition. Panel a
735 reports a bar plot of the average genus-level taxonomic composition obtained for each mammalian
736 taxonomic family. Taxonomic families are grouped by diet. "U. m. of" stands for "Unclassified
737 member of". Panel b shows the bacterial genera with average relative abundance being 2X higher in
738 mammals following a specific diet when compared to the other three considered diets. These taxa
739 are highlighted in green.

740

741 **Figure 3.** Co-variance force-driven network of genera profiled with relative abundance of >5 % in
742 at least a sample. Nodes represent genera included in the analysis and attraction and repulsion
743 forces are proportional to statistically significant co-variances and co-exclusions obtained using the
744 Kendall's tau correlation coefficient. Node size is proportional to the number of correlations. Panel
745 a reports the network with nodes colored based on the predicted modularity class (using 0.6
746 resolution). Panels b and c show the same network with nodes colored to highlight bacterial genera
747 identified as more abundant in a specific diet through analysis of carnivores, herbivores, piscivores
748 and omnivores as well as between only carnivores and herbivores, respectively. Figure numerical
749 legend: *Acinetobacter* (1), *Actinobacillus* (2), *Aeromonas* (3), *Akkermansia* (4), *Alistipes* (5),
750 *Allobaculum* (6), *Alloprevotella* (7), *Anaerococcus* (8), *Asteroleplasma* (9), *Bacillus* (10),
751 *Bacteroides* (11), *Barnesiella* (12) *Bifidobacterium* (13), *Blautia* (14), *Brevundimonas* (15), CAG-

352 (16), *Carnobacterium* (17), *Catenibacterium* (18), *Catenisphaera* (19), *Cellulosilyticum* (20), *Cetobacterium* (21), *Christensenellaceae* R-7 group (22), *Clostridium* sensu stricto 1 (23), *Collinsella* (24), *Comamonas* (25), *Corynebacterium* 1 (26), *Cutibacterium* (27), *Dialister* (28), *Enterococcus* (29), *Epulopiscium* (30), *Erysipelotrichaceae* UCG-002 (31), *Erysipelotrichaceae* UCG-004 (32), *Escherichia-Shigella* (33), *Eubacterium coprostanligenes* group (Ruminococcaceae family) (34), *Faecalibacterium* (35), *Faecalibaculum* (36), Family XIII AD3011 group (Clostridiales order) (37), *Fibrobacter* (38), *Flavobacterium* (39), *Fusobacterium* (40), *Helicobacter* (41), *Ignatzschineria* (42), *Lachnospira* (43), *Lactobacillus* (44), *Lysinibacillus* (45), *Megamonas* (46), *Megasphaera* (47), *Myoides* (48), *Paenibacillus* (49), *Pedobacter* (50), *Peptoniphilus* (51), *Peptostreptococcus* (52), *Photobacterium* (53), *Prevotella* 2 (54), *Prevotella* 7 (55), *Prevotella* 9 (56), Prevotellaceae UCG-001 (57), Prevotellaceae UCG-003 (58), Pseudomonas (59), Psychrobacter (60), Rikenellaceae RC9 group (61), *Ruminiclostridium* 6 (62), Ruminococcaceae NK4A214 group (63), Ruminococcaceae UCG-002 (64), Ruminococcaceae UCG-005 (65), Ruminococcaceae UCG-010 (66), Ruminococcaceae UCG-013 (67), Ruminococcaceae UCG-014 (68), Ruminococcaceae V9D2013 group (69), *Ruminococcus* 1 (70), *Saccharofermentans* (71), *Sarcina* (72), *Shuttleworthia* (73), *Solibacillus* (74), *Solobacterium* (75), *Sphaerochaeta* (76), *Staphylococcus* (77), *Streptococcus* (78), *Streptomyces* (79), *Subdoligranulum* (80), *Succinivibrio* (81) *Sutterella* (82), *Treponema* 2 (83), *Turicibacter* (84), U. m. of Ricketsiales order (85), U. m. of WPS-2 phylum (86), U. m. of Bacteroidales BS11 gut group family (87), U. m. of Bacteroidales order (88), U. m. of Bacteroidales RF16 group family (89), U. m. of Bacteroidales UCG-001 family (90), U. m. of Bacteroidia class (91), U. m. of Burkholderiaceae family (92), U. m. of Caulobacteriaceae family (93), U. m. of Clostridiaceae 1 family (94), U. m. of Clostridiales vadinBB60 group family (96), U. m. of Coriobacteriales order (97), U. m. of Cyanobacteria phylum (98), U. m. of Enterobacteriaceae family (99), U. m. of Erysipelotrichaceae family (100), U. m. of Eukaryota kingdom (101), U. m. of F082 family (102), U. m. of Firmicutes phylum (103), U. m. of

777 Flavobacteriaceae family (104), U. m. of Gammaproteobacteria class (105), U. m. of
778 Lachnospiraceae family (106), U. m. of Lactobacillales order (107), U. m. of Moraxellaceae family
779 (108), U. m. of Muribaculaceae family (109), U. m. of p-251-o5 family (110), U. m. of p-2534-
780 18B5 gut group family (111), U. m. of Pasteurellaceae family (112), U. m. of Peptostreptooccaceae
781 family (113), U. m. of Planococcaceae family (114), U. m. of Prevotellaceae family (115), U. m. of
782 Rhodospirillales order (116), U. m. of Ruminococcaceae family (117), U. m. of
783 Sphingomonadaceae family (118), U. m. of Verrucomicrobiae class (119), U. m. of Weekellaceae
784 family (120), *Vibrio* (121), *Vitreoscilla* (122) and *Yersinia* (123).
785
786 **Figure 4.** Metabolic pathways prediction in Carnivores, Piscivores and Herbivores. Panel a shows
787 the number of pathways detected with abundance >0.001 %. Panels b and c report the sum of the
788 number of all pathways and degradative pathways, respectively, that showed a significantly higher
789 abundance in a specific diet when compared to the other two considered diets observed through the
790 application of an ANOVA post-hoc Bonferroni statistical analysis. Panels d and e display the sum
791 of the number of all pathways and degradative pathways, respectively, with significantly lower
792 abundance in a specific diet when compared to the other two.
793
794 **Figure 5.** Metatranscriptome profiles of carnivores and herbivores. Panel a shows the
795 transcriptional abundance (as a proportion of the total glycobiome) of GH genes with statistically
796 different abundance in carnivores and herbivores. GHs in red show similar abundance in the
797 metagenomes of carnivores and herbivores. Panel b reports the transcriptional abundance (as a
798 proportion of all predicted metabolic pathways) of degradation pathways with statistically different
799 abundance in carnivores and herbivores. Pathways in red displayed similar abundance in the
800 metagenomes of carnivores and herbivores.
801

802 **Figure 6.** Metabolic pathways prediction in Lighter Monogastric, Heavier Monogastric and
803 Polygastric herbivores. Panel a shows the sum of the number of pathways detected with an
804 abundance of >0.001 %. Panels b and c report the sum of the number of all pathways and
805 degradative pathways with significantly higher abundance in a specific class of herbivores. Panels d
806 and e exhibit the sum of the number of all pathways and degradative pathways with significantly
807 lower abundance in a specific class of herbivores. Statistically significant differences were defined
808 by applying the ANOVA post-hoc Bonferroni statistical analysis.

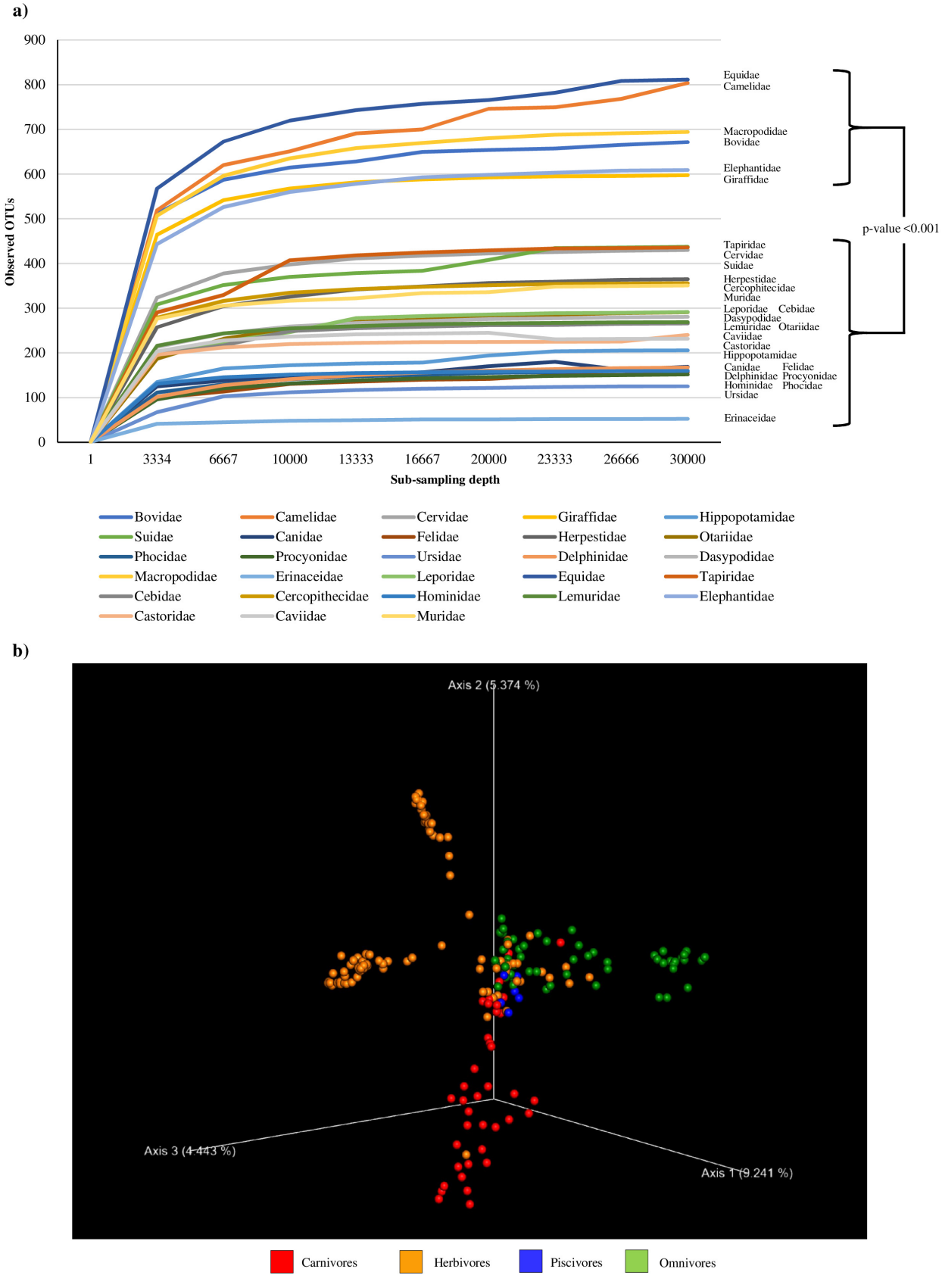

Figure 1

a)

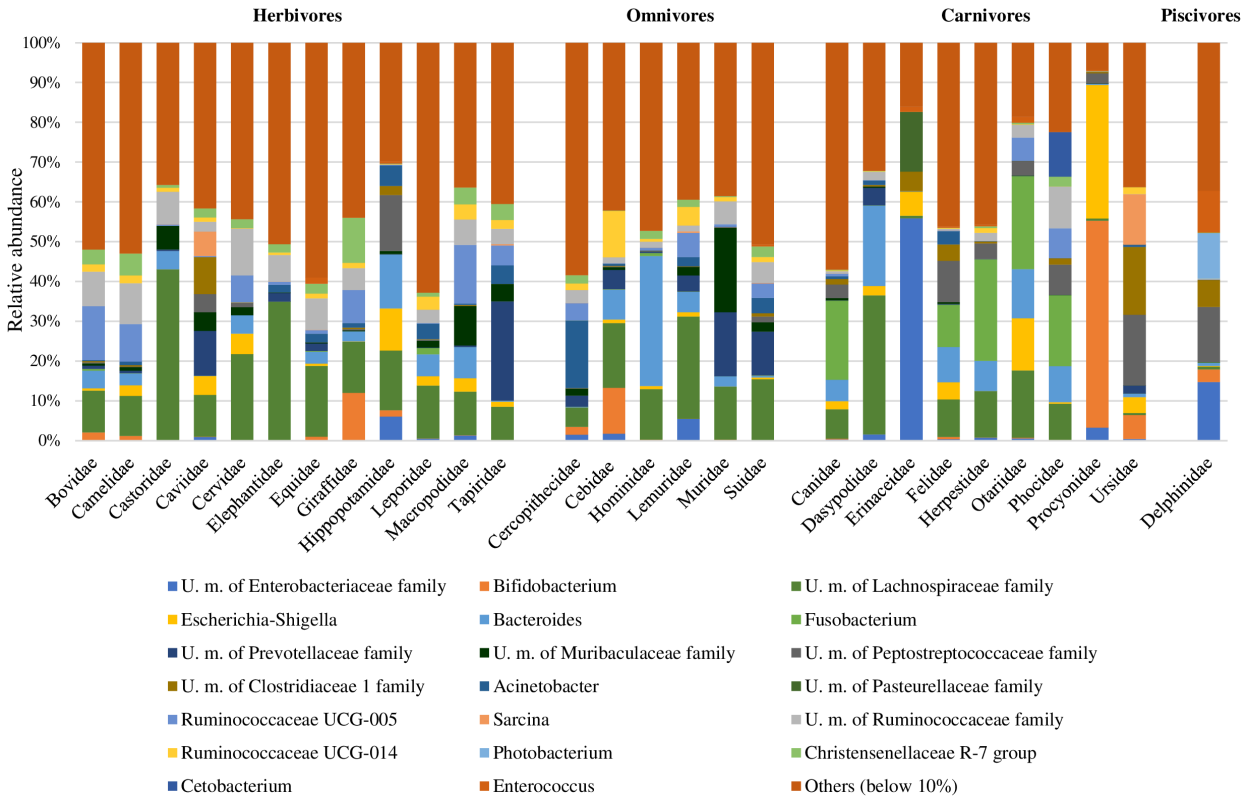

b)

Phylum	Genus	Carnivores	Herbivores	Omnivores	Piscivores	P-value
Actinobacteria	Collinsella	2.08%	0.03%	0.15%	0.09%	0.000
Actinobacteria	U. m. of Coriobacteriales order	1.10%	0.08%	0.16%	0.05%	0.000
Bacteroidetes	Alloprevotella	2.67%	0.73%	0.63%	0.00%	0.000
Bacteroidetes	Rikenellaceae RC9 gut group	0.20%	3.91%	1.36%	0.02%	0.000
Bacteroidetes	U. m. of Muribaculaceae family	0.44%	1.08%	5.13%	0.05%	0.000
Bacteroidetes	U. m. of Prevotellaceae family	0.43%	2.03%	7.05%	0.02%	0.000
Firmicutes	Blautia	2.50%	0.08%	0.50%	0.07%	0.000
Firmicutes	Enterococcus	0.21%	0.42%	0.17%	10.49%	0.000
Firmicutes	Eubacterium coprostanoligenes group (Ruminococcaceae family)	0.45%	2.53%	1.13%	0.06%	0.000
Firmicutes	Faecalibacterium	1.11%	0.19%	2.65%	0.11%	0.000
Firmicutes	Megamonas	1.27%	0.05%	0.13%	0.00%	0.000
Firmicutes	Ruminococcaceae NK4A214 group	0.19%	1.27%	0.58%	0.05%	0.000
Firmicutes	Ruminococcaceae UCG-005	0.84%	6.47%	2.02%	0.07%	0.000
Firmicutes	Ruminococcaceae UCG-010	0.07%	3.63%	0.18%	0.00%	0.000
Firmicutes	Staphylococcus	0.02%	0.01%	0.03%	4.10%	0.000
Firmicutes	Turicibacter	1.83%	0.15%	0.07%	0.46%	0.000
Firmicutes	U. m. of Clostridiaceae 1 family	2.90%	0.58%	0.36%	6.82%	0.004
Firmicutes	U. m. of Clostridiales order	0.11%	2.46%	0.59%	0.06%	0.000
Firmicutes	U. m. of Clostridiales vadinBB60 group family	0.04%	1.12%	0.49%	0.04%	0.003
Firmicutes	U. m. of Lactobacillales order	0.00%	0.00%	0.00%	2.57%	0.000
Firmicutes	U. m. of Peptostreptococcaceae family	5.93%	1.25%	0.53%	13.84%	0.000
Firmicutes	U. m. of Ruminococcaceae family	1.02%	7.07%	3.44%	0.13%	0.000
Fusobacteria	Fusobacterium	15.37%	0.38%	0.28%	0.10%	0.000
Proteobacteria	Actinobacillus	0.01%	0.00%	0.00%	4.37%	0.000
Proteobacteria	Photobacterium	0.00%	0.00%	0.00%	11.49%	0.000
Proteobacteria	Pseudomonas	2.52%	0.37%	1.99%	9.49%	0.010
Proteobacteria	U. m. of Enterobacteriaceae family	0.40%	0.54%	1.52%	14.73%	0.000
Proteobacteria	Vibrio	0.00%	0.00%	0.00%	1.79%	0.000
Verrucomicrobia	Akkermansia	0.07%	1.34%	0.43%	0.05%	0.000

Figure 2

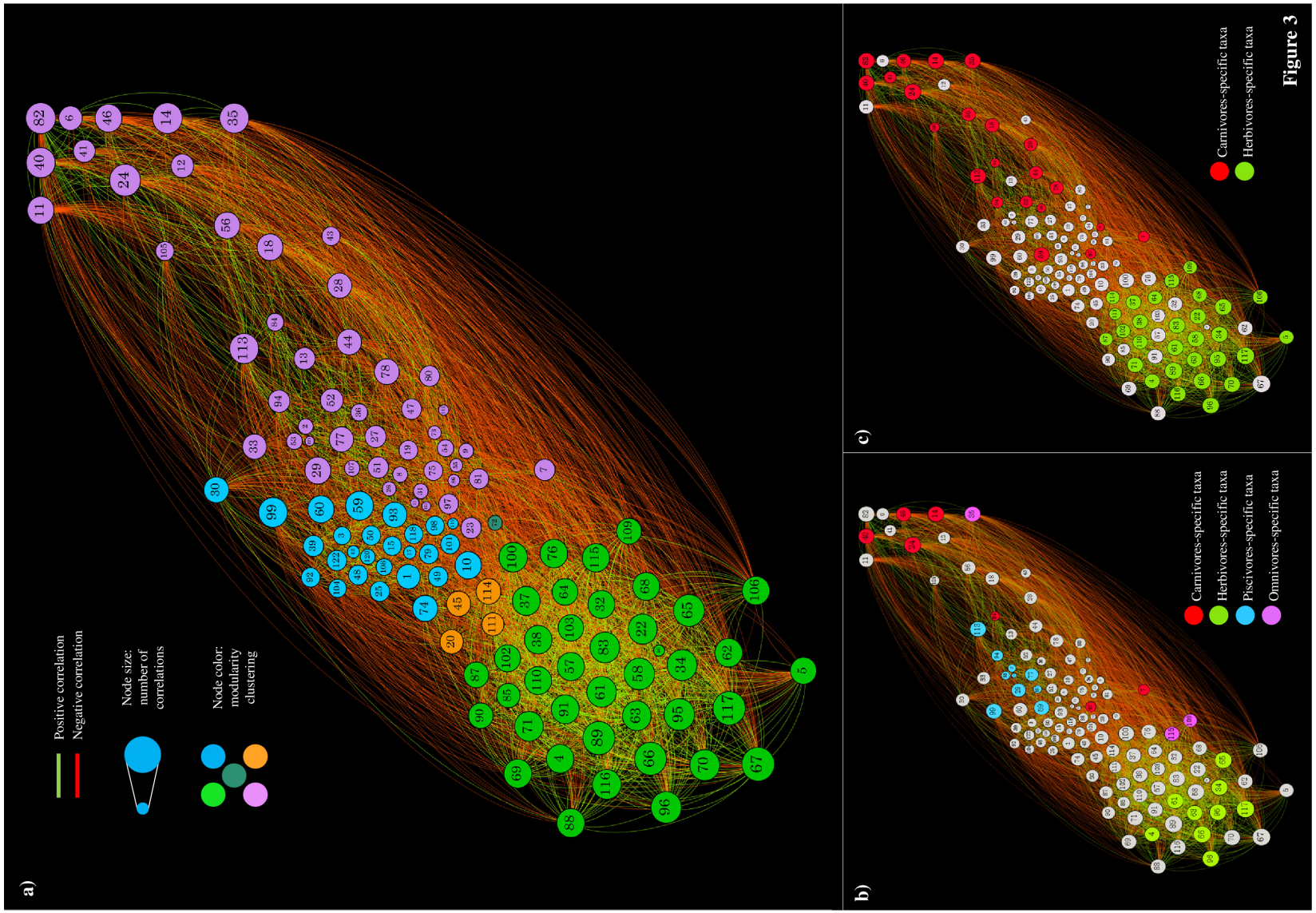

Figure 3

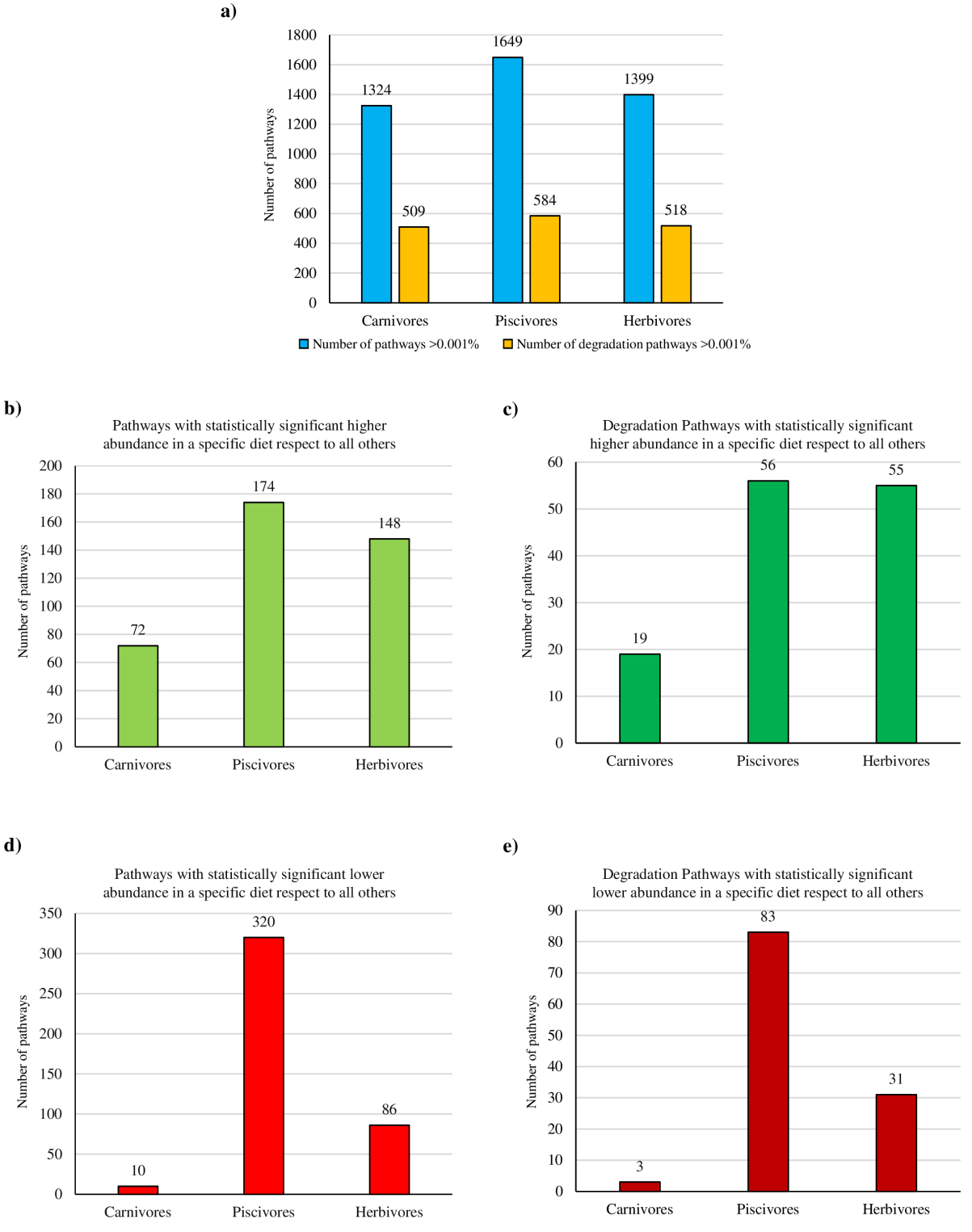

Figure 4

a)

	Canis_lupus_familiaris_1	Felis_silvestris_catus_1	Lynx_lynx_1	Panthera_tigris_1	Capra_hircus_1	Lama_glama_1	Dolichotis_patagonum_1	Equus_ferus_caballus_1	Average abundance in Carnivores	Average abundance in Herbivores	Student's t-test p-value
GH5	0.0244%	0.0201%	0.2997%	0.0314%	0.9828%	0.5239%	2.1412%	1.9077%	0.0939%	1.3889%	0.015
GH9	0.0000%	0.0000%	0.0000%	0.0000%	1.3293%	0.4136%	1.7674%	1.0648%	0.0000%	1.1438%	0.007
GH27	0.2033%	0.0000%	0.0053%	0.0000%	0.3843%	0.1517%	0.1338%	0.3549%	0.0521%	0.2562%	0.049
GH29	0.1139%	0.0402%	0.0210%	0.0000%	0.6363%	0.3447%	0.1246%	0.4880%	0.0438%	0.3984%	0.019
GH30	0.0000%	0.0000%	0.0000%	0.0000%	0.3906%	0.1448%	0.7245%	0.3549%	0.0000%	0.4037%	0.015
GH39	0.0000%	0.0000%	0.0053%	0.0000%	0.0504%	0.1310%	0.4845%	0.4880%	0.0013%	0.2885%	0.047
GH51	0.0163%	0.0402%	0.0158%	0.0026%	0.2898%	0.3516%	0.5999%	1.1535%	0.0187%	0.5987%	0.026
GH66	0.0000%	0.0000%	0.0000%	0.0000%	0.0630%	0.0758%	0.1061%	0.0887%	0.0000%	0.0834%	0.000
GH94	0.1383%	0.0201%	0.2944%	0.0617%	0.8190%	1.3304%	1.2460%	1.2866%	0.1286%	1.1705%	0.000
GH97	0.0000%	0.0000%	0.0000%	0.0000%	0.3969%	0.2550%	0.1200%	0.5768%	0.0000%	0.3372%	0.014
GH105	0.0163%	0.0000%	0.0000%	0.0000%	0.0756%	0.1792%	0.1061%	0.1331%	0.0041%	0.1235%	0.002
GH112	0.0244%	0.0803%	0.0210%	0.0000%	0.1134%	0.0827%	0.0508%	0.1331%	0.0314%	0.0950%	0.043
GH120	0.0000%	0.0402%	0.0000%	0.0000%	0.2268%	0.2275%	0.0923%	0.3993%	0.0100%	0.2365%	0.012
GH130	0.0000%	0.0000%	0.0000%	0.0000%	0.2079%	0.1930%	0.2630%	0.4437%	0.0000%	0.2769%	0.003

b)

	Canis_lupus_familiaris_1	Felis_silvestris_catus_1	Lynx_lynx_1	Panthera_tigris_1	Capra_hircus_1	Lama_glama_1	Dolichotis_patagonum_1	Equus_ferus_caballus_1	Average abundance in Carnivores	Average abundance in Herbivores	Student's t-test p-value
L-citrulline degradation	0.0083%	0.0236%	0.0193%	0.0251%	0.0676%	0.0586%	0.0626%	0.0684%	0.0190%	0.0643%	0.000
naphthalene degradation (aerobic)	0.0011%	0.0000%	0.0002%	0.0000%	0.0133%	0.0103%	0.0071%	0.0080%	0.0003%	0.0097%	0.000
superpathway of beta-D-glucuronide and D-glucuronate degradation	0.0122%	0.0250%	0.0010%	0.0200%	0.0712%	0.0514%	0.0898%	0.0858%	0.0146%	0.0746%	0.000
L-ornithine degradation I (L-proline biosynthesis)	0.0057%	0.0215%	0.0145%	0.0075%	0.0423%	0.0324%	0.0516%	0.0576%	0.0123%	0.0460%	0.000
myo-, chiro- and scyllo-inositol degradation	0.0104%	0.0139%	0.0129%	0.0225%	0.0491%	0.0499%	0.0640%	0.0885%	0.0150%	0.0629%	0.000
D-fructuronate degradation	0.0078%	0.0056%	0.0010%	0.0200%	0.0496%	0.0275%	0.0513%	0.0402%	0.0086%	0.0422%	0.000
K-carrageenan degradation	0.0124%	0.0000%	0.0002%	0.0000%	0.0384%	0.0415%	0.0182%	0.0322%	0.0032%	0.0325%	0.000
superpathway of hexuronide and hexuronate degradation	0.0133%	0.0444%	0.0011%	0.0200%	0.0814%	0.0582%	0.1011%	0.0885%	0.0197%	0.0823%	0.000
superpathway of nicotinate degradation	0.0289%	0.0333%	0.0231%	0.0251%	0.0675%	0.0600%	0.0700%	0.1059%	0.0276%	0.0758%	0.000
L-glutamate degradation VI (to pyruvate)	0.0217%	0.0312%	0.0011%	0.0200%	0.0624%	0.0616%	0.0569%	0.0389%	0.0185%	0.0549%	0.000
nicotinate degradation III	0.0289%	0.0333%	0.0195%	0.0251%	0.0616%	0.0597%	0.0691%	0.1046%	0.0267%	0.0737%	0.001
phenylacetate degradation I (aerobic)	0.0067%	0.0076%	0.0116%	0.0125%	0.0335%	0.0571%	0.0251%	0.0416%	0.0096%	0.0393%	0.001
carbon tetrachloride degradation II	0.0478%	0.0278%	0.0094%	0.0401%	0.2152%	0.2586%	0.1078%	0.1354%	0.0313%	0.1793%	0.001
myo-inositol degradation I	0.0085%	0.0139%	0.0100%	0.0225%	0.0424%	0.0434%	0.0622%	0.0871%	0.0137%	0.0588%	0.001
L-glutamine degradation I	0.8989%	0.4387%	1.0230%	0.7917%	0.1837%	0.2923%	0.2567%	0.3888%	0.7881%	0.2804%	0.001
D-galactonate degradation	0.0033%	0.0028%	0.0000%	0.0000%	0.0271%	0.0082%	0.0297%	0.0161%	0.0015%	0.0203%	0.001
superpathway of microbial D-galacturonate and D-glucuronate degradation	0.0189%	0.0694%	0.0590%	0.0376%	0.1114%	0.0776%	0.1186%	0.1488%	0.0462%	0.1141%	0.001
L-tryptophan degradation II (via pyruvate)	0.0000%	0.0000%	0.0000%	0.0000%	0.0184%	0.0065%	0.0060%	0.0107%	0.0000%	0.0104%	0.001
L-rhamnose degradation I	0.0063%	0.0042%	0.0007%	0.0025%	0.0200%	0.0141%	0.0154%	0.0349%	0.0034%	0.0211%	0.001
beta-D-glucuronide and D-glucuronate degradation	0.0043%	0.0194%	0.0000%	0.0000%	0.0216%	0.0239%	0.0385%	0.0456%	0.0060%	0.0324%	0.001
melibiose degradation	0.0007%	0.0014%	0.0000%	0.0000%	0.0063%	0.0071%	0.0021%	0.0107%	0.0005%	0.0066%	0.001
heme degradation II	0.0070%	0.0118%	0.0034%	0.0025%	0.0460%	0.0171%	0.0442%	0.0778%	0.0062%	0.0463%	0.001
oxalate degradation I / 2-oxobutanoate degradation II	0.0070%	0.0118%	0.0034%	0.0025%	0.0460%	0.0166%	0.0442%	0.0778%	0.0062%	0.0461%	0.002
L-arabinose degradation IV / xylose degradation IV	0.0461%	0.0333%	0.0069%	0.0100%	0.1596%	0.1798%	0.0424%	0.1153%	0.0241%	0.1243%	0.002
benzoyl-CoA degradation II (anaerobic)	0.0209%	0.0292%	0.0034%	0.0075%	0.0618%	0.0442%	0.0523%	0.1140%	0.0152%	0.0680%	0.002
chlorophyll a degradation II	0.0070%	0.0118%	0.0044%	0.0025%	0.0460%	0.0166%	0.0442%	0.0778%	0.0064%	0.0461%	0.002
nucleoside and nucleotide degradation (archaea)	0.0435%	0.0403%	0.0050%	0.0877%	0.0813%	0.2100%	0.1653%	0.1233%	0.0441%	0.1450%	0.002
guanosine nucleotides degradation III	0.0152%	0.0326%	0.0188%	0.0175%	0.0475%	0.0317%	0.0599%	0.0362%	0.0210%	0.0438%	0.002
naphthalene degradation to acetyl-CoA	0.0011%	0.0000%	0.0003%	0.0000%	0.0133%	0.0103%	0.0071%	0.0013%	0.0003%	0.0080%	0.002
4-deoxy-L-threo-hex-4-enopyranuronate degradation	0.0083%	0.0035%	0.0134%	0.0276%	0.0402%	0.0188%	0.0442%	0.0389%	0.0132%	0.0355%	0.002
choline degradation II	0.0054%	0.0076%	0.0005%	0.0050%	0.0007%	0.0002%	0.0002%	0.0000%	0.0046%	0.0003%	0.003
5-hydroxymethylfurfural degradation	0.0000%	0.0000%	0.0000%	0.0000%	0.0244%	0.0142%	0.0145%	0.0013%	0.0000%	0.0136%	0.003
furfural degradation	0.0000%	0.0000%	0.0000%	0.0000%	0.0244%	0.0142%	0.0145%	0.0013%	0.0000%	0.0136%	0.003
oxalate degradation V	0.0000%	0.0000%	0.0001%	0.0000%	0.0008%	0.0005%	0.0002%	0.0013%	0.0000%	0.0007%	0.003
D-glucarate degradation II	0.0000%	0.0000%	0.0000%	0.0000%	0.0003%	0.0005%	0.0005%	0.0000%	0.0000%	0.0003%	0.003
superpathway of glucose and xylose degradation	0.1024%	0.0958%	0.0044%	0.0952%	0.2760%	0.1652%	0.6399%	0.4022%	0.0744%	0.3708%	0.003
quinate degradation II	0.0000%	0.0000%	0.0020%	0.0000%	0.0099%	0.0019%	0.0064%	0.0040%	0.0005%	0.0056%	0.004
chlorophyll a degradation I	0.0070%	0.0118%	0.0182%	0.0025%	0.0471%	0.0166%	0.0449%	0.0791%	0.0099%	0.0469%	0.004
D-sorbitol degradation II	0.0000%	0.0000%	0.0000%	0.0000%	0.0029%	0.0017%	0.0002%	0.0013%	0.0000%	0.0016%	0.004
3,6-anhydro-alpha-L-galactopyranose degradation	0.0046%	0.0028%	0.0000%	0.0125%	0.0286%	0.0130%	0.0338%	0.0121%	0.0050%	0.0219%	0.004
sulfolactate degradation I	0.0017%	0.0000%	0.0003%	0.0000%	0.0130%	0.0163%	0.0030%	0.0295%	0.0005%	0.0154%	0.004
pectin degradation II	0.0000%	0.0000%	0.0000%	0.0000%	0.0008%	0.0006%	0.0035%	0.0027%	0.0000%	0.0019%	0.004
L-tryptophan degradation I (via anthranilate)	0.0000%	0.0000%	0.0000%	0.0000%	0.0060%	0.0074%	0.0016%	0.0013%	0.0000%	0.0041%	0.005
starch degradation III	0.0000%	0.0000%	0.0000%	0.0000%	0.0041%	0.0000%	0.0069%	0.0080%	0.0000%	0.0048%	0.005
L-asparagine degradation I	0.0065%	0.0007%	0.0044%	0.0050%	0.0322%	0.0065%	0.0187%	0.0161%	0.0042%	0.0184%	0.005
D-galacturonate degradation I	0.0087%	0.0354%	0.0001%	0.0125%	0.0489%	0.0310%	0.0762%	0.0335%	0.0142%	0.0474%	0.005
autoinducer AI-2 degradation	0.0000%	0.0000%	0.0000%	0.0000%	0.0018%	0.0019%	0.0009%	0.0000%	0.0000%	0.0012%	0.005
L-lyxose degradation	0.0063%	0.0000%	0.0001%	0.0025%	0.0070%	0.0082%	0.0092%	0.0214%	0.0022%	0.0115%	0.005
superpathway of dimethylsulfoniopropanoate degradation	0.0100%	0.0090%	0.0008%	0.0000%	0.0067%	0.0157%	0.0163%	0.0161%	0.0050%	0.0137%	0.005
2-aminoethylphosphonate degradation I	0.0000%	0.0014%	0.0001%	0.0000%	0.0065%	0.0052%	0.0016%	0.0013%	0.0004%	0.0037%	0.005
superpathway of methanogenesis	0.1128%	0.3096%	0.0143%	0.3783%	0.9144%	0.9832%	0.4444%	0.4612%	0.2038%	0.7008%	0.028

Figure 5

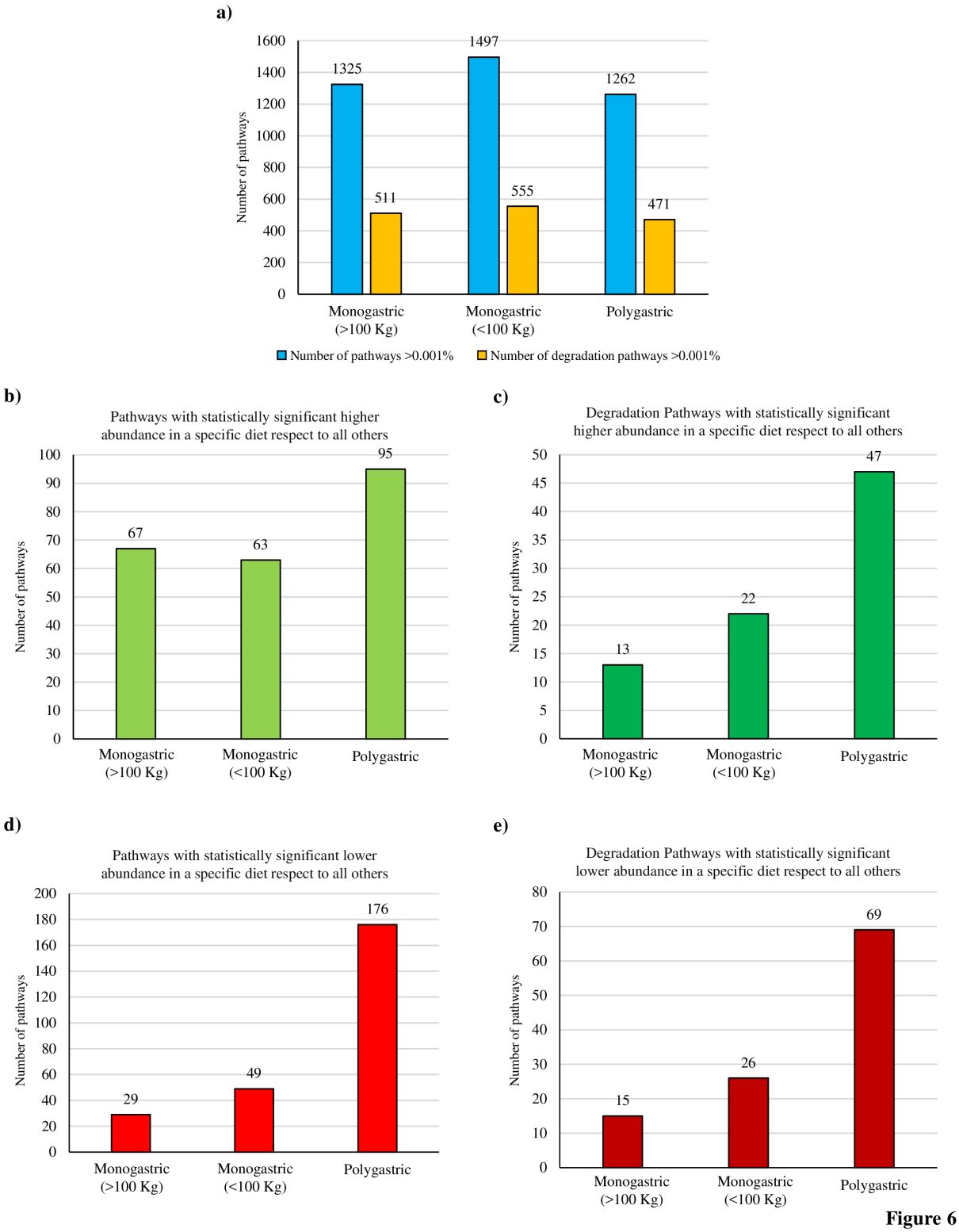

Figure 6